Journal of the European Ceramic Society

Recycling of bottom ash from biomass combustion in porcelain stoneware tiles: effects on technological properties, phase evolution and microstructure

--Manuscript Draft--

Manuscript Number:	JECESOC-D-22-00524R1
Article Type:	Full Length Article
Keywords:	bottom ash; Microstructure; porcelain stoneware; technological properties; waste recycling
Corresponding Author:	Sonia Conte CNR-ISTEC Italian National Research Council-Institute of Science and Technology of Ceramic Materials Faenza (RA), ITALY
First Author:	Sonia Conte
Order of Authors:	Sonia Conte
	Daniele Buonamico
	Tommaso Magni
	Rossella Arletti
	Michele Dondi
	Guia Guarini
	Chiara Zanelli
Abstract:	This work aims to evaluate the use of bottom biomass ash as an alternative raw material in porcelain stoneware bodies. For this purpose, ash coming from a biomass thermoelectric power plant in Emilia-Romagna (Italy) was selected and its chemical, mineralogical and thermal properties determined. Data indicated its technological role as a flux, so it was introduced in a porcelain stoneware batch in partial replacement of feldspars and experimented at laboratory scale. A bottleneck, relative to the rheological behavior of the slips, was overcome by a slight deflocculant increase. The powder compacts were fired from 1000 to 1220°C in order to follow the evolution of the technological properties, phase composition (XRPD-Rietveld) and microstructure (SEM). The introduction of ash allowed to lower the firing temperature by 20°C, while keeping the technological properties comparable with those of the benchmark. Moreover, the mineralogical and microstructural data revealed different sintering kinetics.

National Research Council of Italy
istec Institute of Science and Technology for Ceramics

Faenza, May 5th, 2022

To the Editor of ***Journal of the European Ceramic Society***,

Dear Editor,

please find attached the new version of the manuscript entitled ***Recycling of bottom ash from biomass combustion in porcelain stoneware tiles: effects on technological properties, phase evolution and microstructure*** by Sonia Conte, Daniele Buonamico, Tommaso Magni, Rossella Arletti, Michele Dondi, Guia Guarini, Chiara Zanelli.

On behalf of all the authors, I testify that the manuscript has not been published or under editorial review for publication elsewhere.

All the reviewers' and editor's suggestions were considered for the new manuscript and commented in a "*response-to-reviewers*" letter, while the corrections were reported in the text with different colors: gray text with strikethrough for deleted parts and text highlighted in yellow for additions

We hope that now our paper will be suitable for publication on ***Journal of the European Ceramic Society***.

Yours sincerely,

Sonia Conte

V.A.T. 02118311006
C.F. 80054330586
Via Granarolo, 64 – 48018 FAENZA (RA) - Italy
Phone: +39 0546 699711-Fax +39 0546 46381
e-mail: istec@istec.cnr.it PEC: istec@pec.cnr.it

Summary of Novel Conclusions

Fully comprehensive study on the feasibility of the biomass bottom ash recycling in porcelain stoneware bodies, through the evaluation of the main technological properties' variations and the study of the influence of ash introduction on phase composition and microstructure at different stage of sintering.

Response to Reviewer's comments

Reviewer #1:

The Authors present their manuscript (JECESOC-D-22-00524) focused on the technological feasibility of the biomass ash recycling in porcelain stoneware bodies, with special emphasis on all the industrial steps of the ceramic tiles production (milling - granulation - shaping - drying - firing). The use of biomass ash as a renewable raw material for the production of porcelain stoneware bodies constitutes a sustainable alternative of high economic and environmental interest. From a practical point of view, the work is very interesting and stands out for seeking to identify possible bottlenecks along the route of industrial porcelain stoneware processing. This topic is significant and of broad international interest. The manuscript is well structured and contains important scientific analyses. The results and conclusions are well presented and deserve to be published. Thus, I recommend the acceptance of it.

Reply: We are glad of this result and would like to thank you the referee.

Editors' comments:

1. Please check the quality of the graphs! Fig. 3 is of poor resolution. Fig. 6 and 9 do not have scale markers on X and Y-axis.

Reply: thank you, we checked all the figures, Fig. 3 has been modified and now is of better resolution. We also modified fig 6 and 9 adding the scale markers.

2. Use professional scale markers for the SEM micrographs and remove the automatically generated figure caption at the bottom.

Reply: thank you for your suggestion, we modified all the SEM micrographs by removing the automatically generated figure caption and adding professional scale markers.

3. The conclusion section is very long! References should not be used in the conclusion section! Batch and sample numbers should be avoided (C0 and C4). The final paragraph: "Anyway, ... investigations" should be removed from the conclusion section, since that is not really a conclusion from this manuscript.

Reply: the conclusion section has been shortened; references were removed from the conclusion section, as well as sample numbers; the final paragraph: "Anyway, ... investigations" were moved in the results and discussion section.

Recycling of bottom ash from biomass combustion in porcelain stoneware tiles: effects on technological properties, phase evolution and microstructure

Sonia Conte[1*], Daniele Buonamico[2], Tommaso Magni[2], Rossella Arletti[2], Michele Dondi[1], Guia Guarini[1], Chiara Zanelli[1]

[1]CNR-ISTEC, National Research Council, Institute of Science and Technology for Ceramics, Via Granarolo, 64-48018, Faenza, Italy

[2]Department of Chemical and Geological Science, University of Modena and Reggio Emilia, Via Giuseppe Campi, 103-41125 Modena, Italy

ABSTRACT

This work aims to evaluate the use of bottom biomass ash as an alternative raw material in porcelain stoneware bodies. For this purpose, ash coming from a biomass thermoelectric power plant in Emilia-Romagna (Italy) was selected and its chemical, mineralogical and thermal properties determined. Data indicated its technological role as a flux, so it was introduced in a porcelain stoneware batch in partial replacement of feldspars and experimented at laboratory scale. A bottleneck, relative to the rheological behavior of the slips, was overcome by a slight deflocculant increase. The powder compacts were fired from 1000 to 1220°C in order to follow the evolution of the technological properties, phase composition (XRPD-Rietveld) and microstructure (SEM). The introduction of ash allowed to lower the firing temperature by 20°C, while keeping the technological properties comparable with those of the benchmark. Moreover, the mineralogical and microstructural data revealed different sintering kinetics.

Keywords: bottom ash, microstructure, porcelain stoneware, technological properties, waste recycling.

***Corresponding author**: Sonia Conte

mail: sonia.conte@istec.cnr.it,

permanent address: Via Granarolo, 64, 48018 Faenza RA, Italy

phone: +390546699711

fax: +39054669979

1. INTRODUCTION

The manufacture of ceramic tiles is globally steady, with a production around 13 billion square meters in the latest years [1], implying a constant demand for raw materials attaining an estimated global consumption beyond 300 million tons per year [2]. On the other hand, the progressive depletion of the main mineral deposits that this production rate imposes, is forcing the ceramic industry to look for suitable substitutes, which guarantee specific technological properties to the finished product. The efforts of the ceramic industry in the latest years to replace natural raw materials with secondary ones, was also driven by marketing reasons supported through green certificates [3-5], like Ecolabel and the LEED credits (The Leadership in Energy and Environmental Design; WGBC, 2022 [6]), and the standard on the sustainability of ceramic tiles (ISO 17889, 2021 [7]). To make the production completely sustainable in the long run, in view of the transition to a circular economy, but ensuring the high technological performances of the product, represents a challenge for the ceramic industry [8]. Although to date this industry has proven to be able to recycle its own processing residues very efficiently, the use of waste from other sources is currently rather limited. Among the materials that could be tested as secondary raw material in ceramic production, biomass combustion ashes represent an opportunity, since biomass is increasingly replacing fossil fuel in thermal power plants and, for this reasons, ashes are locally available in significant amount.

In principle, silicate ceramics are good waste acceptors since they are composed of heterogeneous bodies: a mixture of various minerals that undergo phase transformations during processing, especially at the firing stage. This is favorable for the waste incorporation because a highly heterogeneous mix is intrinsically prone to accommodating extraneous components. At any rate, a certain waste is increasingly tolerated as far as its technological behavior resembles those of conventional raw materials [9-12].

Nowadays, what is lacking to promote the widespread recourse to recycled raw materials is the knowledge about the effect of a specific waste in ceramic tile manufacturing. In this context, a recent work of Zanelli and co-workers [12] overviewed the effect of waste recycling on technological behavior and technical performance of ceramic tiles. Such a technological outlook regarding bottom ashes from biomass combustion revealed that there is little information about the technological behavior during the pre-firing processes (from body preparation to pressing and drying) while the firing step has been more investigated [13-23]. Despite the almost absence of studies on the pre-firing steps, it emerges that they are the more critical, due to the high susceptibility of the ash to moisture (tendency to cementation), which can cause several problems in the storage and handling of this waste [12].

In general, bottom ashes from biomasses are the product of a combustion by thermal power plants to produce energy by burning organic matter. Combustion processes give rise to residues that can be basically distinguished between a quantitatively predominant coarse-grained bottom ash [24-25] and fly ash that generally has a very fine particle size [26-27]. Combustion of biomasses produces different ashes, since sources can be extremely varied: rice husk [14,17,21,28-29], coffee husk [30-33], sugar cane bagasse [16,19,22,34], palm oil and sago [23,35-36], cereal straw and stalk [13,15], wood and forestry wastes [18,37], fish bone [38-39] and leather waste [20]. Biomass ashes exhibit therefore a considerably variable composition, primarily depending on the source (Table 1). In general, plant-based ashes are siliceous materials, poor in alumina and rich in P_2O_5 with respect to ceramic bodies, while the content in alkalis and alkali-earths is rather high, especially some ashes peak over 20% CaO or over 10% K_2O (Tables 1 and S1, supplementary material).

Table 1. Chemical composition of ashes from combustion of biomasses of different sources.

% wt.	**Sugarcane bagasse ash** [16,19,22,34]	**Sago ash** [36]	**Palm oil ash** [35]	**Coffee husk ash** [33]	**Rice husk ash** [28]	**Rice straw ash** [14,29]	**Fish bone ash** [38]	**Wood ash** [18]	**Biomass bottom ash** [This work]
SiO_2	62.25	68.03	66.91	13.86	90.23	73.68	0.77	42.85	43.10
TiO_2	0.80	0.03	-	0.26	0.13	-	0.04	-	0.45
Al_2O_3	6.88	6.93	6.44	4.47	1.07	0.22	0.61	-	8.71
Cr_2O_3	-	0.04	-	-	-	-	-	-	0.02
Fe_2O_3	5.34	0.76	5.72	1.63	0.27	0.31	0.06	6.13	4.45
MgO	2.50	2.39	3.13	13.22	0.18	1.68	0.88	0.65	4.40
CaO	6.76	14.88	5.56	35.19	0.39	2.22	59.26	27.93	27.58
MnO	0.12	0.65	-	0.15	-	0.60	-	2.40	0.14
CuO	-	-	-	-	-	0.01	-	-	0.03
ZnO	-	-	-	-	-	0.04	0.02	0.44	0.01
SrO	-	-	-	0.25	-	0.01	0.17	-	0.11
BaO	-	-	-	-	-	0.06	-	-	0.04
Na_2O	0.41	1.35	0.19		-	0.39	0.74	0.67	1.20
K_2O	7.68	1.35	5.20	11.76	1.36	13.12	0.11	4.54	5.36
P_2O_5	1.41	1.66	3.72	9.85	3.83	2.56	36.84	-	1.44
SO_3	1.08	2.02	0.33	0.28	-	1.42	0.30	-	0.04
Cl	-	-	-	0.12	-	0.99	0.08	-	0.01
L.o.I.	7.72	-	2.30	9.82	3.83	1.84	-	13.73	3.17

Laboratory experimental data relative to the firing behavior and technical performance of ceramic tiles containing different kind of biomass ashes, indicated that they seem generally adequate to replace fluxes or fillers in low proportion (≤10wt%) in porcelain stoneware. A significant reduction of firing temperature is reported, without influencing too much the technical properties and the tile microstructure. This occurred with ashes from coffee husk, rice straw, and sugarcane bagasse, which are characterized by high alkali values [13-14,16,19,30,32]. Positive results were registered also with other wastes, like palm oil ash, as a substitute of quartz in a porcelain batch, which led to an increase

in compressive strength [23]. Essentially, there are evidences that these wastes play as a strong flux, reducing the temperature of maximum densification, in accord with a composition rich in Fe, Na, K and poor in Si and Al. A darker colour after firing and a fast decrease in bulk density were observed for increasing ash amount [12-14,17]. The literature agrees that the use of biomass ash can lead to properties matching the standards for porcelain stoneware tiles, with a recommended recyclable amount in most cases between 5 and 10%. Anyway, to date, the technological feasibility of ashes recycling can be affirmed only in relation to the firing behaviour. In fact, the technical constraints of the pre-kiln processes have not been adequately assessed and there may be technological pitfalls. Moreover, detailed information unravelling the effect of the substitution on the phase and microstructure transformations occurring at the different stages of the firing are not available. This is a crucial point in understanding the reasons of eventual changes during sintering.

The goal of this work is therefore to evaluate the technological feasibility of the biomass ash recycling in porcelain stoneware bodies, in relation to all the industrial steps of the ceramic tiles production (milling – granulation – shaping – drying – firing), in order to identify possible bottlenecks along the manufacturing line. This was possible by simulating the industrial cycle at the laboratory scale, verifying the effect of the ash introduction not only on the fired products but also on the semi-finished ones. In addition, a detailed characterization of the phase composition and microstructure of the fired bodies at different temperatures was carried out to understand the way by which the biomass ash affects the viscous sintering.

2. EXPERIMENTAL

In the present work bottom ash from biomass combustion (BBA), coming from a thermoelectric power plant in Faenza, Emilia-Romagna (Italy), was exploited as an alternative raw material in porcelain stoneware bodies. These bottom ashes represent the combustion product of woody material, grass, pomace and a mix of tree essences, treated at a declared combustion temperature between 700 and 1000°C. They are classified by the CER code (European waste catalog, directive 75/442/EEC) CER 10 01 01: Waste produced by thermal power plants and other thermal plants, defined as non-hazardous materials [40]. Bottom ashes are, by definition, coarse-grained, so their particle size distribution was determined by sieving test (sieves sequence 4, 2, 1, 0.5, 0.25, 0.125, 0.063 mm). Moreover, the ash was characterized from the chemical, mineralogical, and thermal point of view. The chemical composition was determined by XRF-WDS (PW 1480, Philips) and reported in Table 1, while the mineralogical composition by XRPD analysis (X'PERT PRO, PANalytical). The thermal behavior of the ash was studied by thermogravimetric analysis (TGA-DTG) performed under flowing air on powder (~15 mg) up to 1050°C, using a TG/DTA 320U thermobalance and 20°C/min heating

rate, alumina crucibles and Pt–Pt10Rh thermocouples. The fusibility was determined by hot stage microscopy (HSM Misura 3- 402ES/3, Expert System Solution) with a cycle of 10°C/min up to 1600°C. The results indicated a technological role of BBA as a fluxing component in substitution of feldspars. Therefore, four different porcelain stoneware batches were designed: a benchmark without ash named C0 and three bodies with increasing BBA amount up to 6wt%, named C2-C4-C6 (Table 2). The maximum amount of ash (6wt%) was decided on the basis of literature results [12-23] and experimental tests. Indeed, preliminary laboratory tests indicated that the introduction of this ash brings about a worsening of rheological behavior of the slips (increase of viscosity measured by the time of flow through Ford cup). This bottleneck can be easily managed in batches containing ash up to 6wt% by a deflocculant increase (0.6wt% instead of 0.3wt%). On the other hand, a higher amount of ash would entail an excessive deviation from the technological behavior of conventional raw materials.

Table 2. Formulations of the batches and their chemical composition (wt%) calculated considering the contribution by weight of each raw material.

%wt		**C0**	**C2**	**C4**	**C6**
PLASTIC COMPONENT	Ball clay A	20	20	20	20
	Ball clay B	20	20	20	20
FLUXES	Sodic feldspar	35	34	33	32
	Potassic feldspar	10	9	8	7
FILLER	Quartz-feldspathic sand	7	7	7	7
	Silica sand	8	8	8	8
BIOMASS BOTTOM ASH	BBA	0	2	4	6
SiO_2		69.77	69.23	68.69	68.15
Al_2O_3		18.87	18.69	18.51	18.33
TiO_2		0.60	0.61	0.61	0.62
Fe_2O_3		0.54	0.62	0.71	0.79
CaO		0.44	0.97	1.51	2.05
MgO		0.35	0.43	0.51	0.59
K_2O		2.25	2.29	2.32	2.36
Na_2O		4.03	3.93	3.84	3.74
P_2O_5		<0.01	0.03	0.06	0.09
MnO		<0.01	<0.01	0.01	0.01
Loss on Ignition (LOI)		3.16	3.20	3.25	3.30

The four designed batches were experimented at the laboratory scale, simulating the industrial tile-making process. Before adding it to the batches, the ash was ground using a hammer mill with a 500 μm grid. Then all the raw materials were ball milled in a porcelain jar using dense alumina grinding media, 40% water (by weight of the slip) and 0.6% deflocculant (sodium tripolyphosphate) by weight of dry batch, for 20 minutes. The slips were oven dried, de-agglomerated (hammer mill with grid of 500 μm) and manually granulated (sieve 2 mm, moisture ~8wt%). Powders were compacted with a

hydraulic press (40 MPa) into 110×55×5 mm tiles, dried in an electric oven at 105 ± 5°C overnight and characterized for: particle size distribution (ASTM C958), springback (i.e., $100(L_p-L_m)/L_m$, where L_p is the length of the pressed tile and L_m is the length of the mold), green and dry bulk density (weight/volume ratio), as reported in Table 3.

Powder compacts were fast fired in an electric roller kiln (ER15; Nannetti, Faenza, Italy) at seven different maximum temperature ranging from 1000 to 1220°C (T_{max}: 1000, 1100, 1130, 1160, 1180, 1200, 1220°C), with a thermal cycle of about 60 min cold-to-cold and 5 min of dwell time at T_{max}. Technological properties, determined after firing the specimens at the different T_{max}, are: linear firing shrinkage (i.e., $100(L_m-L_f)/L_m$ where L_f is the length of the fired tiles and L_m is the length of the mold), water absorption, bulk density and open porosity (ASTM C373) (Table S2, supplementary material). CIE ‐ Lab colorimetry (ISO 10545 ‐ 16, MSXP ‐ 4000; Hunterlab, Reston, VA, USA) of sintered tiles was also performed and the L^*, a^*, and b^* values reported in Table S3 (supplementary material).

The sintering behavior of the four batches was investigated by in-situ experiments on specimens (approximately 5x5x5 mm) cut from the pressed compacts. Experiments were carried out by optical thermo-dilatometry (TA, ODP868, Germany) with a firing schedule consisting of heating ramp (40°C/min) up to 1180°C and testing the body stability by increasing temperature by steps of 10°C up to 1220°C (with 5 min dwell time at every step).

X-Ray powder diffraction patterns were collected on powdered fired tiles after the addition of 10wt% of Al_2O_3 standard. The samples were laterally loaded on an Al-sample holder and the patterns were collected using a X'PERT PRO, PANalytical with θ-θ geometry and CuKα radiation, in the 0–110°2θ range, with counting times of 120 seconds for each step. The combined RIR-Rietveld method, which enables the quantitative phase analysis (QPA) and the calculation of both the crystalline and amorphous fractions [41] was performed by using the GSAS software [42] with the EXPGUI interface [43]. The results and details of the refinements are reported in Table S4 (supplementary material).

The microstructural evolution of the four batches fired at temperatures corresponding to specific stage of the sintering process (start, intermediate stage, maximum densification and overfiring) was observed by scanning electron microscopy (JSM-6010 LA InTouchScope, graphite sputtered polished surface, JEOL, USA).

3. RESULTS AND DISCUSSION

3.1. Characterization of biomass bottom ash

The grain size curve of the biomass bottom ash is shown in Figure 1, by which a d_{50} of 2.05 mm can be derived. Such a grain size distribution is slightly coarser than those observed for wood biomass ashes by Modolo and co-workers [44] and Cabrera and co-workers [45], which appear, on average, finer. Moreover, the maximum diameters of the particles exceed the size of 4 mm, in line with the literature studies cited above.

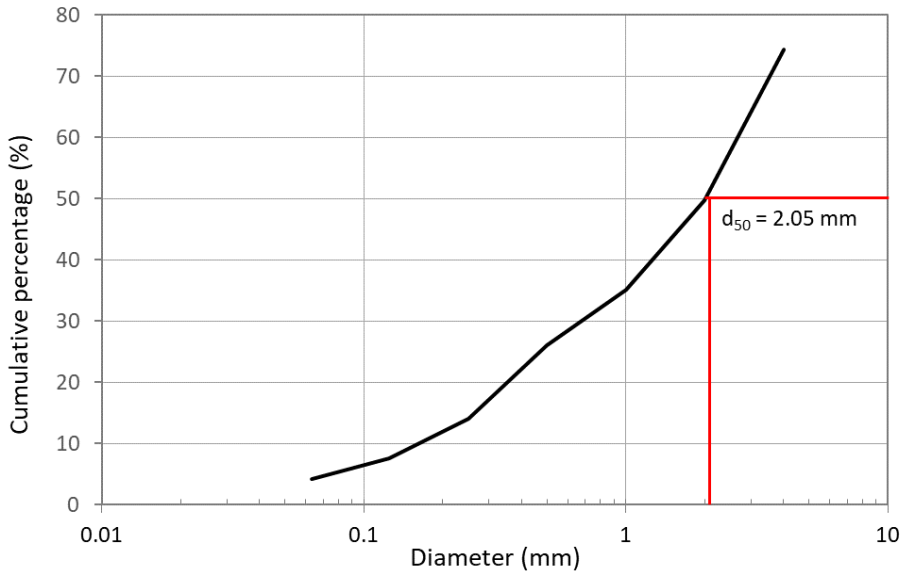

Figure 1. Grain size distribution of BBA

From the chemical point of view, the BBA are generally mainly composed by Si, Ca, Al, Fe, Mg, K and P [46], even if the relative concentration of a specific element is function of the biomass from which the ashes originated (Table 1). The BBA object of this study shows a chemical composition quite compatible with those relative to ashes coming from the combustion of agricultural and forest residues and from a mix of them [18,44,47-48]. Compared to the fluxes it has replaced, the bottom ash shows peculiar features, with a lower content of SiO_2 and Al_2O_3 (~43 and ~9%wt, respectively) and higher amount of CaO, Fe_2O_3, MgO and P_2O_5 (Table S1).

The qualitative XRPD analysis of BBA indicates the presence of quartz, K-feldspar, leucite, wollastonite, cristobalite, melilite, calcite and portlandite (Figure 2), also in this case mostly matching the literature data relative to biomass bottom ashes [49-50].

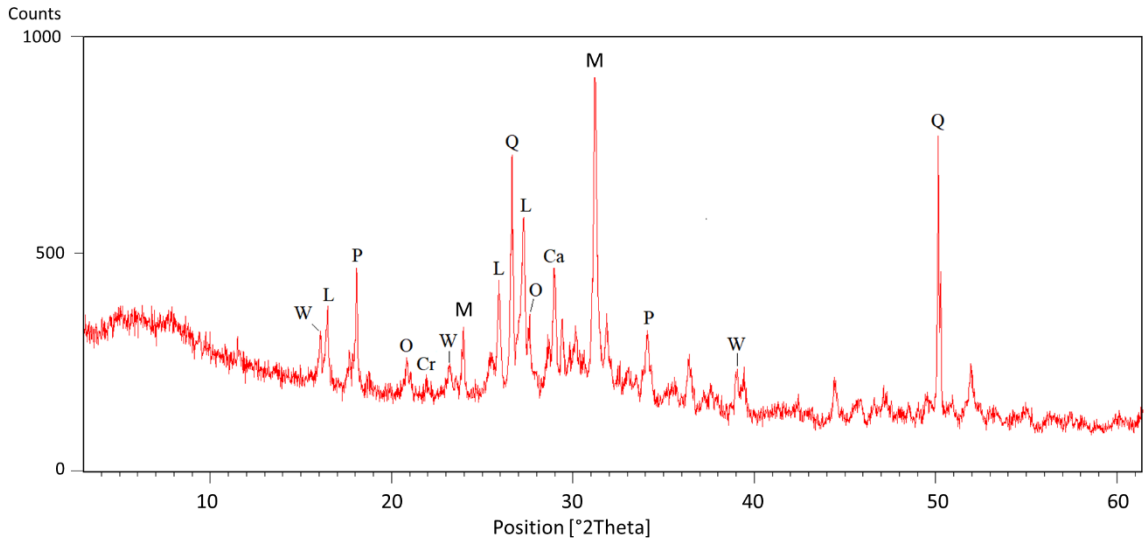

Figure 2. XRPD pattern of the biomass bottom ash under study. Q= Quartz, M=melilite, W= Wollatonite, L=Leucite, P=Portlandite, Cr=Crystobalite, Ca=Calcite, O= Ortoclase.

The behavior of the BBA as a function of temperature was evaluated through the combination of thermogravimetric analysis (TG-DTG) and by hot-stage microscopy (HSM). As shown in Figure 3, the weight loss of the ash is about 3wt%, mirroring the value obtained as loss on ignition (Table 1). It occurs mainly in two steps, both associated to very weak endothermal reactions. The first is between 300 and 500°C (~0.5%, DTG peak at ~480°C), and the second is between 550 and 770°C (~2.5%, DTG peak at ~750°C). The former can be attributed to thermal decomposition of portlandite and the latter to calcite.

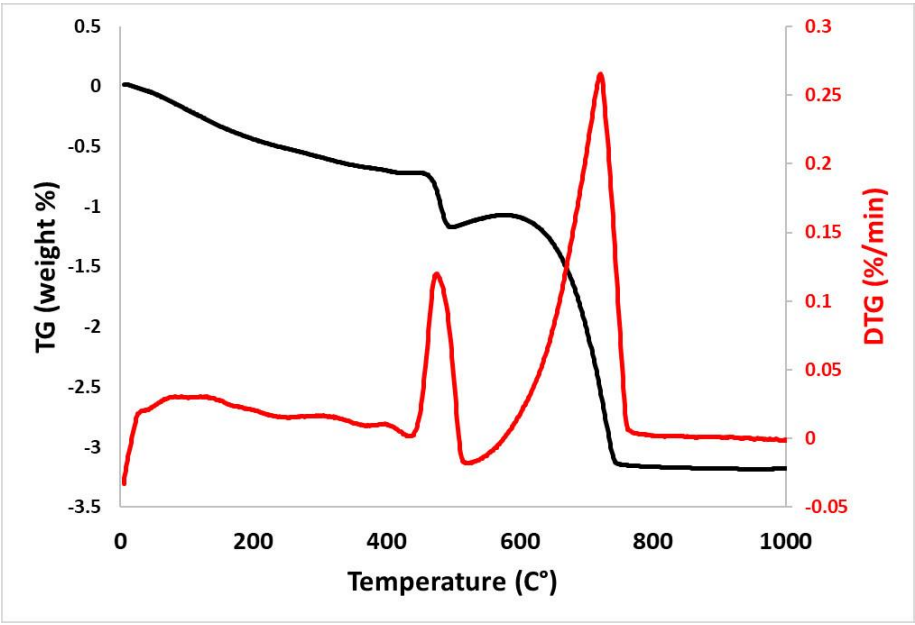

Figure 3. TGA-DTG curves of BBA

The fusibility degree of the BBA is demonstrated by the softening and melting temperatures, as obtained by HSM, which are close to 1210 and 1240°C, respectively. Such characteristic temperatures can be compared with those of various ceramic fluxes through the fusibility chart reported in Figure 4, which depicts the fields of fusibility from very low to very high and a zone of high risk of bloating (related to higher contents of iron oxide) [51]. The BBA is characterized by a very high fusibility and a low risk of bloating.

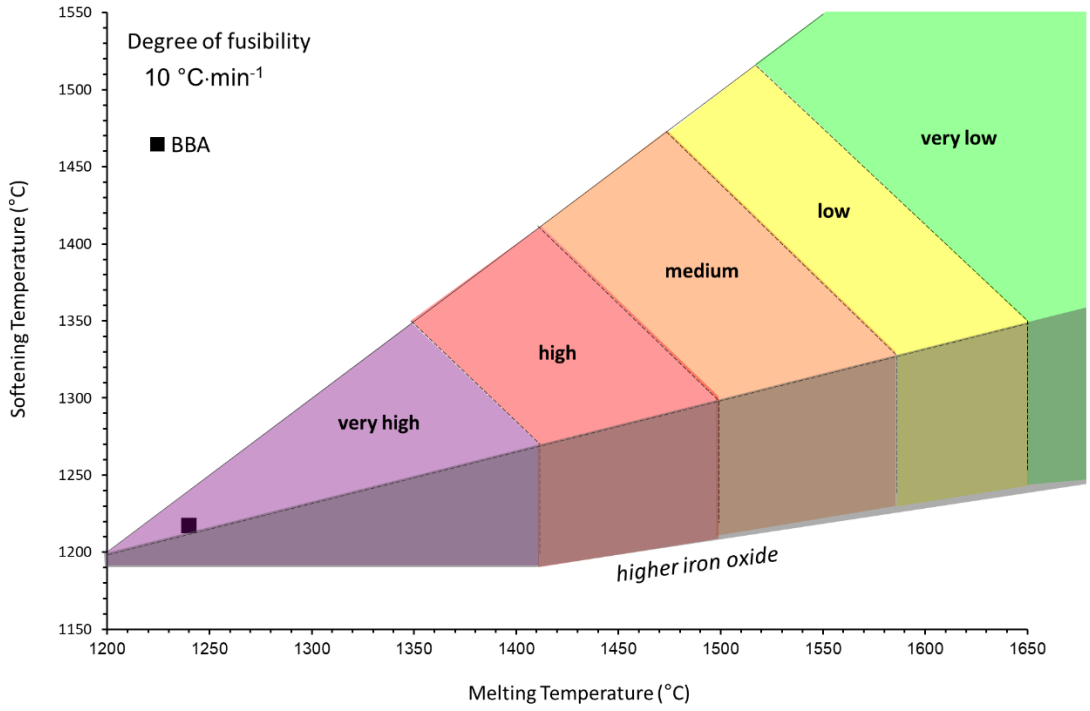

Figure 4. Fusibility of BBA according to the chart after [51].

It should be remembered that the chemical and mineralogical composition, as well as the thermal behavior, of biomass bottom ashes is extremely variable, depending not only on the biomass of origin but also on the processes with which were generated. The characterizations of the ashes themselves before their employ are therefore of fundamental importance. On the other hand, these ashes are classified by the CER code (European waste catalog, directive 75/442/EEC) as non-hazardous materials, and, in force of this and their properties, they represent an excellent candidate for in-depth technological investigations.

3.2. Technological properties of semi-finished and finished porcelain stoneware tiles

The BBA had a significant impact in the first step of production, i.e., the wet milling. The ash led to a worsening of the rheological properties of the slip with a relevant increase in viscosity. Anyway, this bottleneck was easily overcome thanks to a slight addition of deflocculant (from 0.3 to 0.6wt%). This correction allowed an adequate wet milling, obtaining bodies with very similar particle size

distribution, with a median particle diameter between 3.3 and 3.9 μm (Table 3 and Figure 5), that matches usual values in ceramic tile production.

Table 3. Technological properties of unfired products.

Property	unit	C0			C2			C4			C6		
Particle size d_{50}	μm	3.3	±	0.0	3.8	±	0.0	3.8	±	0.0	3.9	±	0.0
Springback	cm/m	0.50	±	0.02	0.47	±	0.02	0.45	±	0.01	0.44	±	0.02
Green bulk density	g/cm^3	2.066	±	0.003	2.130	±	0.013	2.149	±	0.012	2.145	±	0.005
Dry bulk density	g/cm^3	1.936	±	0.004	1.993	±	0.003	2.008	±	0.012	1.993	±	0.004

The presence of the ash did not modify the technological behavior of porcelain stoneware bodies during the granulation, shaping and drying steps. Small variations were observed also for the technological properties of semi-finished products (Table 3). Specifically, a slight increase in both green and dry bulk density in bodies containing ash implies an improvement in the degree of compaction due to the presence of BBA. On the other hand, the springback, even if slightly decreased, is still in the range usually accepted in the industrial practice, i.e., 0.3–0.6 cm/m [52].

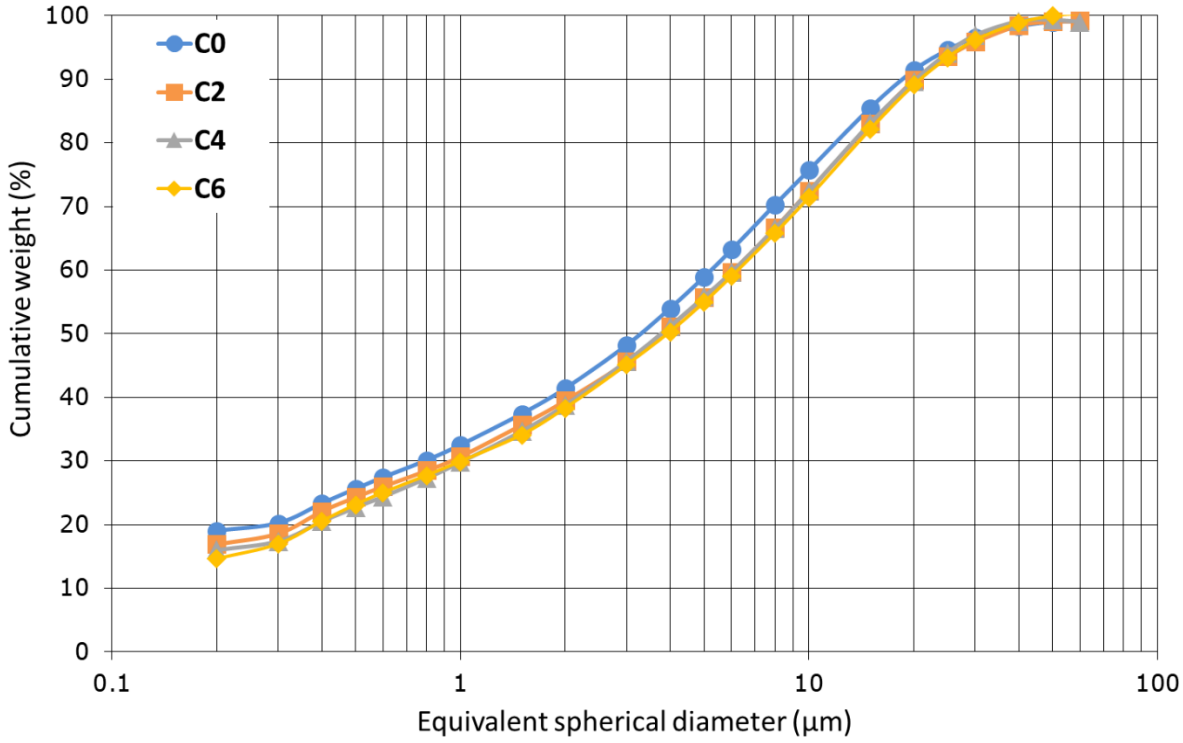

Figure 5. Particle size distribution of batches C0-C2-C4-C6.

Technological properties determined after firing at different maximum temperatures are reported in Figures 6-7 and Table S2, supplementary materials. At variance with the semi-finished products, the BBA significantly influenced the firing behavior. The linear shrinkage decreased with the amount of ash (Figure 6).

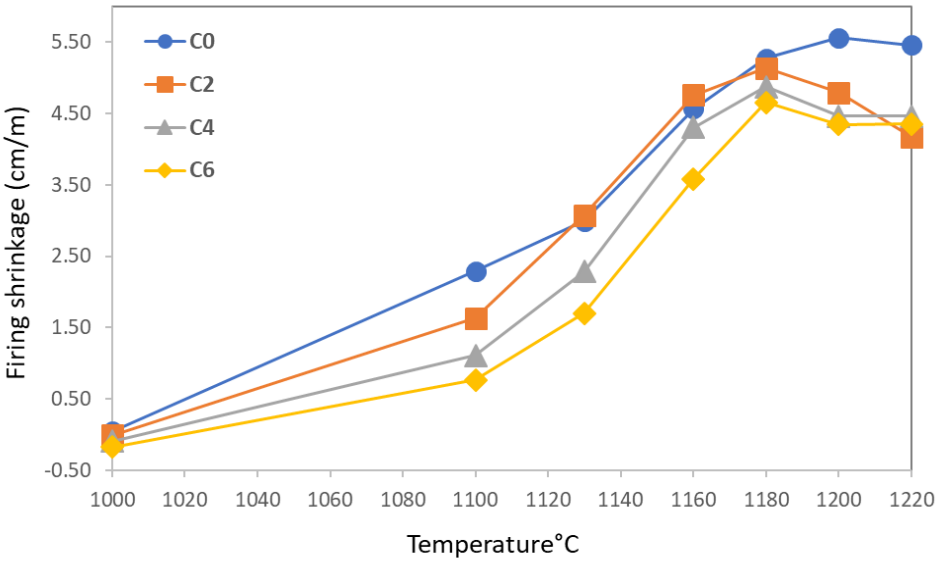

Figure 6. Linear firing shrinkage of finished products fired at different temperatures. Standard deviations within the symbol size.

Actually, increasing BBA from 2 to 6%wt led to a progressive reduction of linear shrinkage values, less pronounced for batch C2. Moreover, the waste-bearing bodies reached their maximum shrinkage at 1180°C, showing similar values among them and also close to the benchmark. Beyond this temperature, they exhibit an expansion of the ceramic bodies, while the waste-free body C0 continued to shrink up to 1200°C, reaching the highest value of the set (5.56 cm/m), and remained stable even at 1220°C.

Taking into account water absorption and bulk density, it is possible to observe their evolution over a wide range of temperatures (Figure 7 and Table S2).

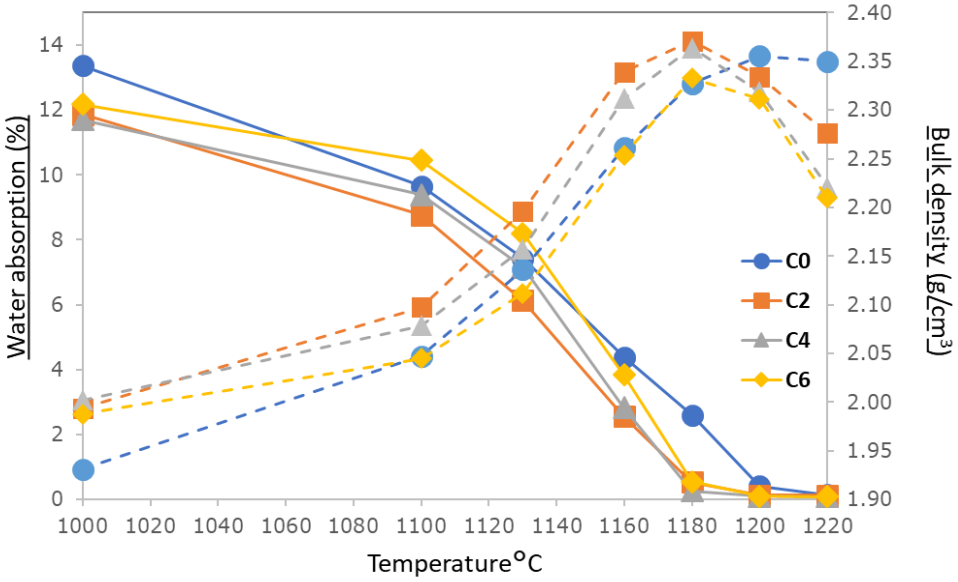

Figure 7. Gresification curves for batches C0-C2-C4-C6. Standard deviations within the symbol size.

At 1000°C, the batches containing ash are characterized by a slightly higher bulk density with respect to the benchmark, corresponding to a lower water absorption, likely inherited from the higher bulk density of unfired compacts (Table 3). At 1100°C, it is no longer possible to observe a clear distinction in behavior between the waste-bearing batches and the reference, mostly because of the sample C6, characterized by a delay in densification in the 1100-1130°C range, with respect to batches C2 and C4. Starting from 1100°C onwards there is, for all the samples, a change in the slope of the curves with a significant increase in density and a corresponding decrease in water absorption, indicating an increase in sintering kinetics. At 1180°C the batches with BBA reached their maximum density, with values very similar for C2 and C4, slightly lower for C6; at this same temperature they also show values of water absorption ≤0.5%, which allow to define 1180°C as their adequate firing temperature. The decreasing of the maximum bulk density with increasing amount of ashes has been observed also with the introduction of rice straw and rice husk ashes [14,17], bagasse ashes [16] and coffee husk ashes [30]. Even if at 1200°C the water absorption is lower for C2-4-6 bodies, they suffer from a significant loss of density, which, in accordance with the linear shrinkage data, indicates an expansion of the ceramic body, more accentuated at 1220°C. On the other hand, for the benchmark the sintering process is still going on at 1180°C, as witnessed by the high water absorption (2.6%) and still increasing bulk density values. Indeed, for this batch the densification is accomplished at 1200°C, i.e., 20°C higher than samples containing ash. Nevertheless, it is worth noting that C0 is characterized by a more pronounced stability even at the highest temperature with respect to the other batches.

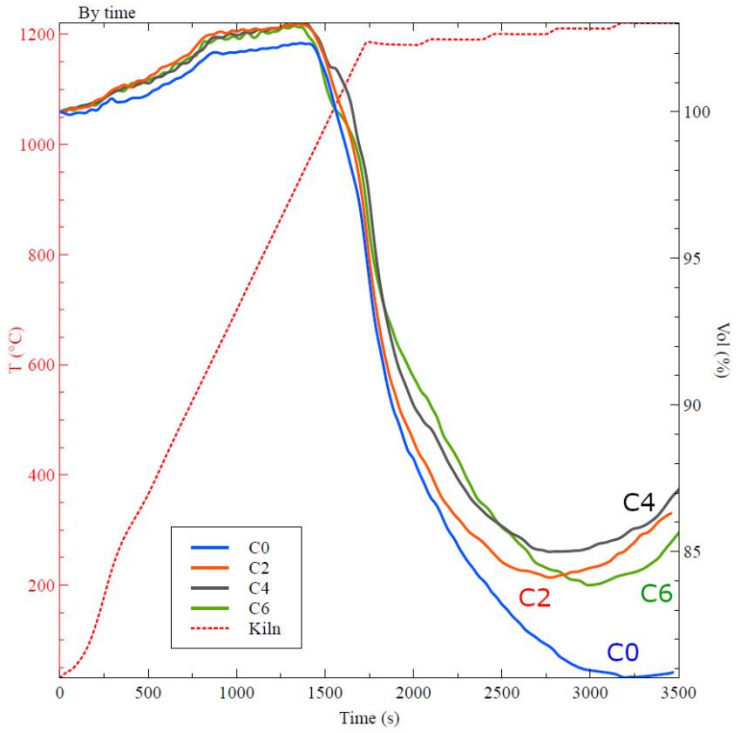

Figure 8. HSM stability curves of C0-C2-C4-C6 bodies.

Indeed, in Figure 8, it is possible to notice that the C0 remained stable once reached the maximum densification, still going on to densify up to at 1220°C, where a hint of instability can be glimpsed. Otherwise, for the bodies with ash, once reached the maximum densification there is a rapid expansion of the specimens (inferred from the inversion of the curves, that indicates an increase in volume), related to de-sintering processes. These bloating phenomena, corroborated by the decrease in shrinkage, bulk density and increase in closed porosity (Table 3 and SEM micrographs), were observed also in porcelain tiles containing rice straw ashes [14,29], especially when present in high amount (i.e., 60wt%), and are generally caused by the greater content in gas-releasing substances (Fe_2O_3, chlorides, also as LOI) coming from the ash.

For as concerns the colour of the tiles (Table S3, supplementary materials), considering those fired at the maximum densification temperature (1180°C for C2-4-6 and 1200°C for C0), the presence of ash induced very small variations. The main changes concern the L^* parameter: all the ash-bearing bodies turned a bit darker (from 73 of the benchmark down to 67 L^*). At the same time, they exhibit slightly higher values of a^* so resulting a little redder, and, just in the case of C6, slightly higher values of also b^*, resulting yellower than body C0. These colour changes can be related with the variation of iron content, since the ash introduction implies a little increase in the total iron amount of the batches (Table 2).

3.3 Phase composition of fired porcelain stoneware tiles

Porcelain stoneware is typically composed of quartz and feldspar remnants, and neo-formed mullite, embedded in an abundant vitreous phase [53-54]. The phase composition of the four bodies fired at the seven different temperatures (28 samples) are summarized in Figure 9 and reported in Table S4 (supplementary material).

The presence of quartz decreases as a function of the increasing temperature in all the batches, indicating its partial melting, with a rather steady rate over 1100°C. This general tendency is expected, since it is known that quartz dissolution has an exponential dependence on firing temperature [55]. In the ash-free C0, the quartz dissolution rate increases later with respect to the ash bearing samples and quartz remained in a slightly higher amount at the end of the ramp. More in detail, the fast dissolution of quartz in C0 started from 1130°C with a significant drop in its amount up to 1180°C, of around 5wt%; then its content decreased with a slower rate. The batch with the minor content of ash, C2, really kept a constant rate of quartz dissolution along the ramp, while the trends of C4 and C6 are almost overlapping, apart from a first considerable reduction in C6 between 1100 and 1130°C, of around 4wt% of quartz. It can be inferred from these results that the increasing introduction of ash moderately affects the evolution of quartz. Actually, the relative variation of its contents in all the

batches – from the starting temperature up to the higher – is quite small, with a decrease of 7.3-7.5wt% for C0-C2 and 8.2-8.7wt% for C4-C6.

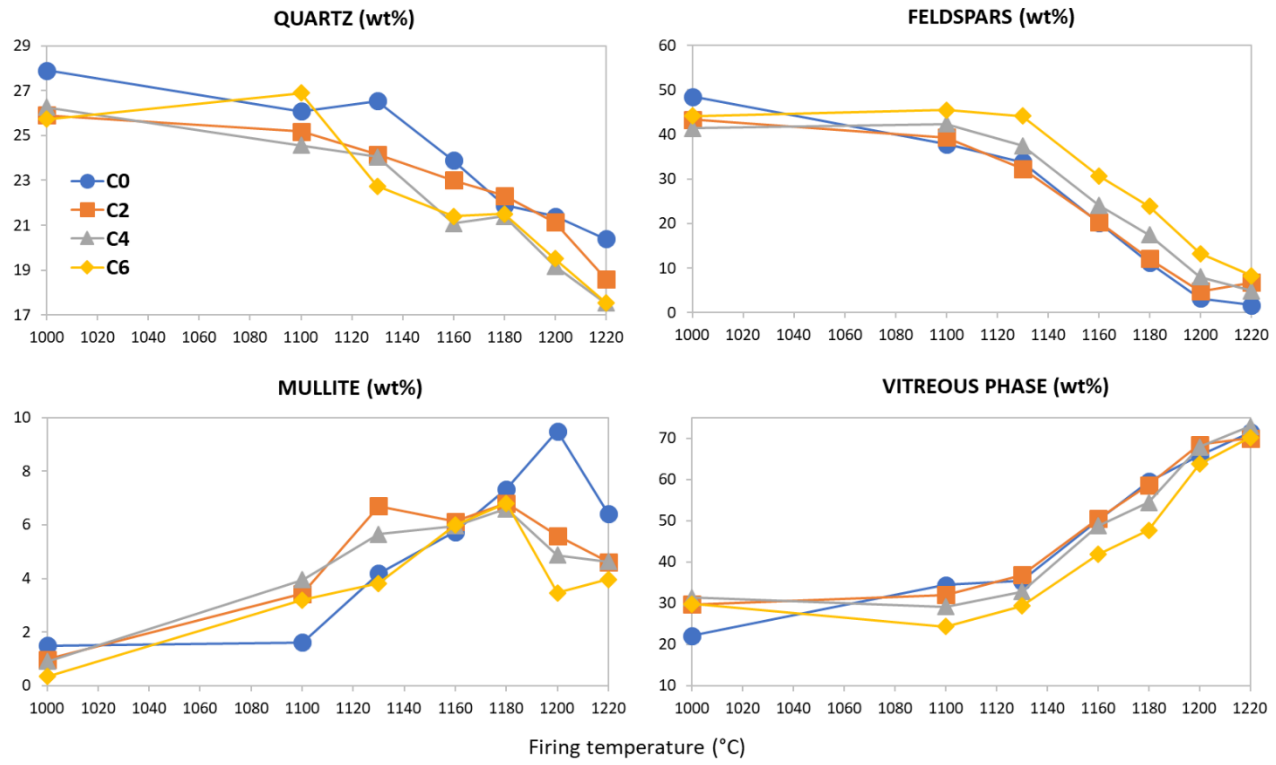

Figure 9. Phase composition of C0-C2-C4-C6 batches. Standard deviations within the symbol size.

Feldspars – plagioclase plus K-feldspar – are the main ingredients of porcelain stoneware, playing the role of fluxing agents. In between 1000 and 1130°C, the contents of feldspars remained more stable the more ash is added, while in the C0 batch their content decreased fairly regularly in this range. Specifically, for batch C0 there is a significant drop in this temperature span, with a dissolution of ~15wt% of feldspars. Considering the waste-bearing batches, C2 with a decrease of 11wt%, shows an intermediate behavior between C0 and the other batches C4 and C6. In these latter samples, in fact, the amount of feldspars shows a very slow decrease for C4 (4wt%), while a stable content with no variation is observed for C6, sign of no dissolution in this temperature range. Starting from 1130°C onwards there is, for all the samples, a change in the slope of the curves with a significant increase in the melting kinetics, with a drop of ~30-35wt% of feldspars for all the bodies, in the range 1130-1220°C. Samples containing ash, as the temperature increased, retained more plagioclase than sample C0, with a direct correlation between the amount of ash introduced in the bodies and the residual plagioclase. Indeed, at the end of the ramp, at 1220°C, C0 shows a content of feldspar of ~2wt% *versus* those of the ash-bearing batches ranging from ~5 to 8wt%. This phenomenon sheds light on the behavior of the ash, beyond its fluxing role. BBA melted in place of the feldspars, allowing a greater amount to be preserved up to the maximum firing temperatures. Despite no data on

quantitative mineralogical composition of ash-bearing batches are available in the literature, an analogous behavior has been observed for porcelain stoneware containing glassy wastes [56] and also strong fluxes [57]. Conte and co-workers [56] reported that porcelain stoneware bodies with 20wt% of different kinds of glassy waste (bottle, lamp, screen...) retained, after firing, more feldspars than the reference body. Similarly, also batches with strong fluxes – such as ulexite, colemanite, wollastonite and diopside in amount ≤10wt% – preserved a slightly higher amount of feldspars with respect to the standard [57].

Mullite begins its crystallization at a temperature of about 1000°C, the growing rate of this phase is higher in the first range of temperature (1000-1100°C) for the waste-bearing bodies with respect to C0, which shows a delay of about 100°C. This delay is somehow compensated by a faster rate of crystallization in the range 1100-1200°C, which is higher than that showed by the waste-bearing bodies in the span 1000-1180°C. The maximum mullite content is reached for all the samples at the maximum densification temperature, i.e., 1180°C for C2-C4-C6 and 1200°C for the C0, even if in different amount (~7wt% for the ash-bearing bodies *versus* 9.5wt% for the benchmark). After reaching the maximum densification temperature, the mullite appears to be unstable and its content slightly decreased in all the batches. At the best of our knowledge, no quantitative data on mullite contents are available for ceramic batches with ashes. Nevertheless, we can compare our data with those of porcelain stoneware obtained after the addition of glassy waste [56] and strong fluxes [57]. Results indicated that the introduction of raw materials rich in alkali and alkali-earths inhibits the mullite formation, decreasing its contents at the temperatures of maximum densification, if compared to the respective benchmarks.

Due to the breakdown of phyllosilicates, the incipient melting of feldspars and the partial melting of quartz, the amorphous phase increased with firing temperature, particularly from 1130°C onwards, when its amount passed from ~30-37wt%, to ~70wt% at 1220°C. The amount of glassy phase present in the bodies is different at the temperatures of maximum densification (1180°C, about 50-60% for samples with ash; 1200°C, 66% for C0), while it is almost the same for all samples at the maximum tested temperature (1220°C). Overall, the trend of the vitreous phase suggests a limited effect of BBA up to 4wt% and a more appreciable decreasing in content in C6.

Quantitative mineralogical data allowed to identify a temperature range characterized by massive phase transformations, whom gave rise to the sintering by viscous flow of the ceramic body. Indeed, between 1100 and 1130°C, the bulk density curves became steeper (Figure 7), indicating the acceleration of the densification process. Overall, the mineralogical data suggest that the introduction of BBA did not deeply influence the evolution of the phases. However, the observed variations of quartz, mullite and feldspars between the reference body and those with ash have some implications.

The mechanism that guarantees the high temperature stability of the porcelain stoneware bodies requires the presence of a quartz and mullite skeleton inside a peraluminous melt. Any dissolution of the quartz skeleton would lead to a decrease in the viscosity of the mass, but is counterbalanced by the increasing viscosity of the liquid phase, due to the increase in its silica content [54]. If the skeleton is made up of feldspars, their dissolution, with release of alkali and alkali-earth, would lead to a drop in viscosity of the liquid phase and no counterbalancing effect would occur. This is the undesired phenomenon that limits the use of peralkaline raw materials (molar ratio $Al_2O_3/Na_2O+K_2O+CaO<1$).

3.4 Microstructure of fired porcelain stoneware tiles

To investigate the microstructure at various temperatures, corresponding to different sintering stages, scanning electron microscope analyses were carried out. Four different significant temperatures were selected: *i)* 1000°C for the start of the sintering process, corresponding to small tile size variation up to 1100°C; *ii)* 1130°C for the intermediate stage, characterized by formation of glassy ponds, accounting for most densification up to the temperature of maximum density [58]; *iii)* the maximum densification of bodies at 1180°C for C2, C4, C6 and at 1200°C for C0; *iv)* 1220°C for overfiring.
At the lowest temperature considered (1000°C, Figure 10), all samples exhibit characteristics of un-sintered bodies. Specifically, a highly crystalline appearance is observed, characterized by several crystals with sharp edges, resulting from grinding, which represents the starting assemblage of feldspars and quartz grains dispersed into a fine-grained matrix that includes clay minerals and porosity.

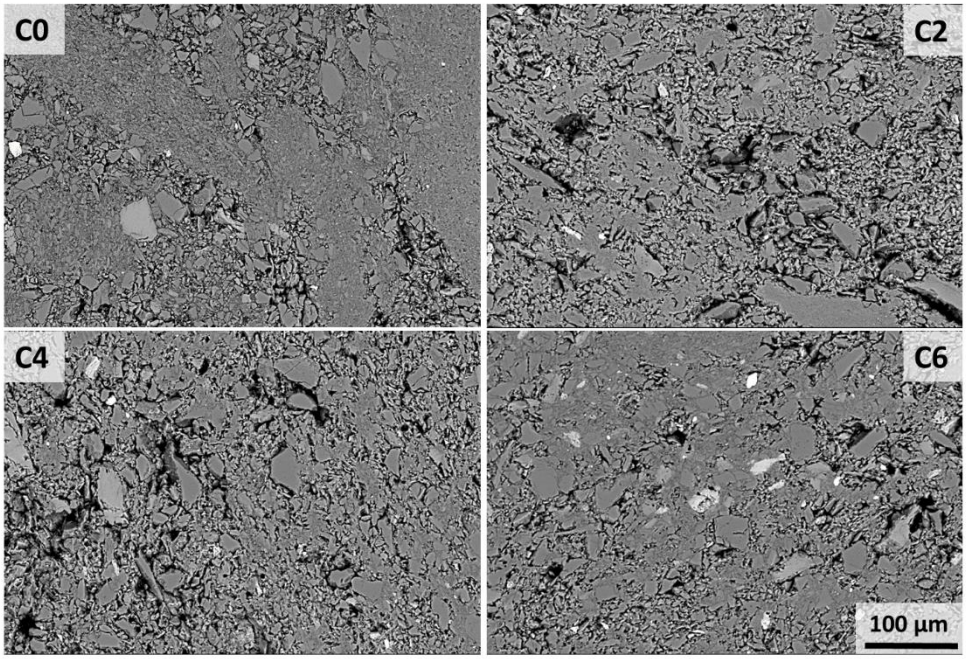

Figure 10. SEM-BS micrographs of C0-C2-C4-C6 bodies fired at 1000°C (scale bar = 100 µm).

Figure 11 shows a detail of an image collected on the C6 sample, accompanied by EDS spectra collected on some points of interest. The high-contrast grain, analyzed in spectrum 1, is rich of iron, while the grain analyzed in point 2 is compatible with a K-feldspar, and grains at points 3-4 are quartz.

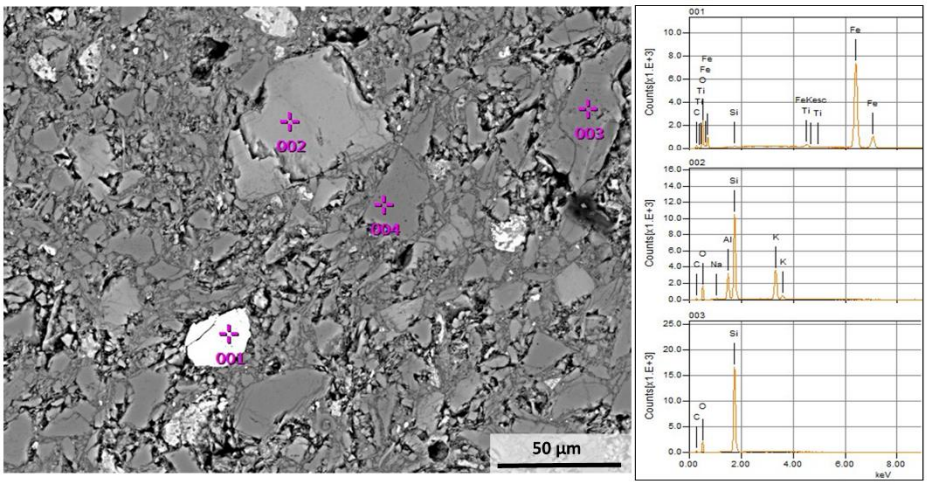

Figure 11. SEM-BS micrographs of C6 fired at 1000°C: iron oxide, microcline, quartz (scale bar = 50 µm).

At 1130°C (Figure 12) the C0 sample is still mainly characterized by crystals with a defined shape, while for the other bodies, the increase in temperature led to a significant loss of angularity and the formation of necks between the various grains, which suggest the occurrence of a liquid phase and the melting of feldspars and ash. As it can be seen from the graphs of phase evolution (Figure 9), it is indeed at this temperature that an abundant melting began, leading to the fast increase of the vitreous phase.

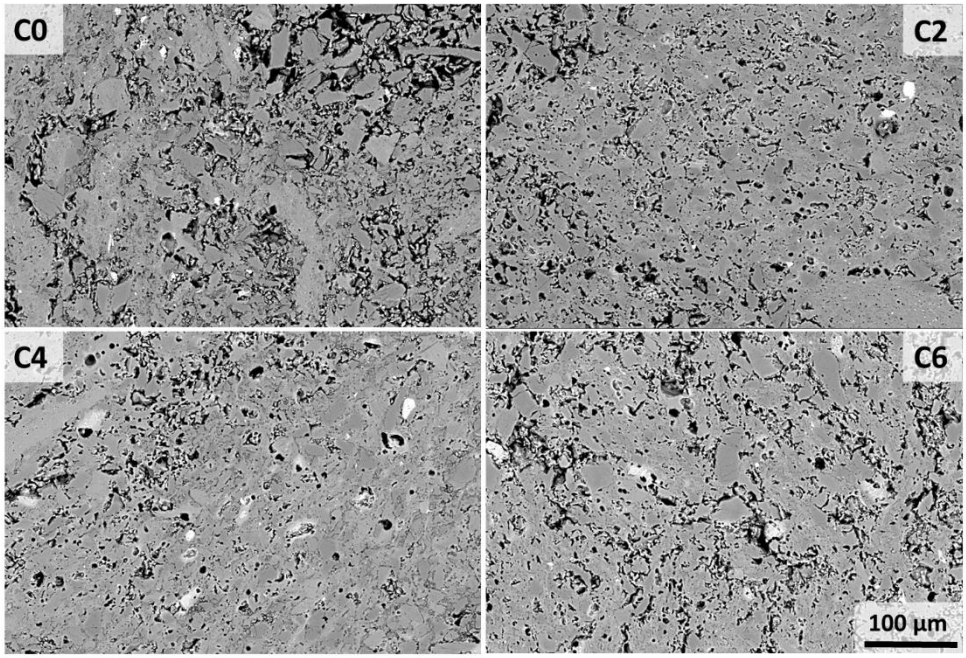

Figure 12. SEM-BS micrographs of C0-C2-C4-C6 bodies fired at 1130°C (scale bar = 100 µm).

At the temperature of maximum densification (Figure 13) all the batches show a compact microstructure with relics of quartz and feldspars crystals, rounded isolated pores (from a few μm up to ~20 μm in diameter) and irregularly shaped pores, presumably inherited from powder compaction defects. Crystals and pores are dispersed in an abundant vitreous phase (liquid at high temperature), which promoted the sintering process by wetting the mineral particles and reducing the voids, so increasing the bulk density of the ceramic tile. These microstructural features are typical of sintered porcelain stoneware [54,57]. In detail, it is possible to observe that the reference batch shows a lower volume of pores with respect to the other samples. Pores are, on average, also smaller in size.

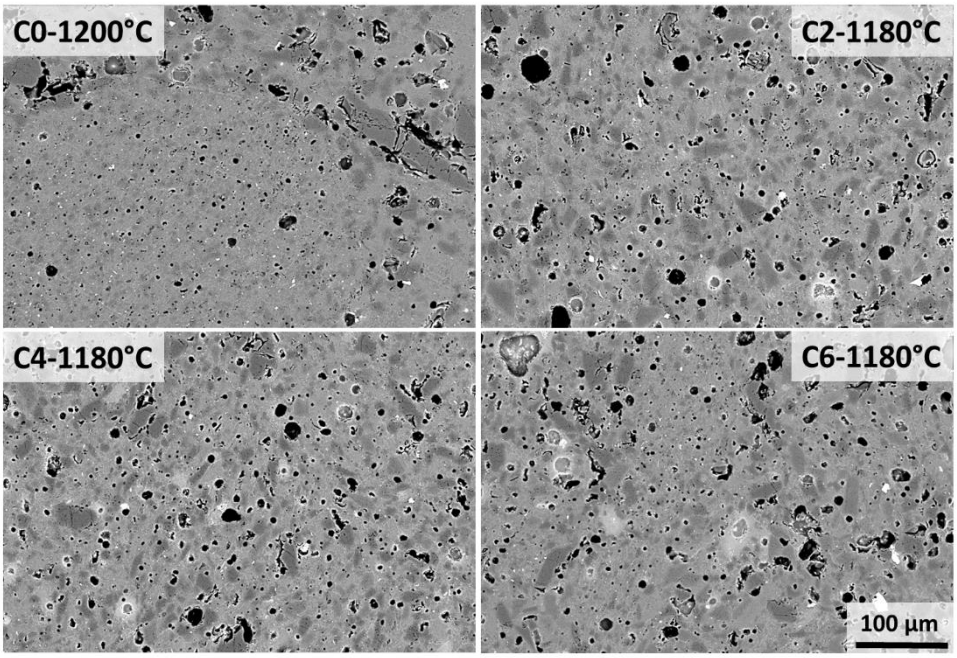

Figure 13. SEM-BS micrographs of bodies fired at T_{md} (scale bar = 100 μm).

Similar features, with increasing in closed porosity – quantity and size – related to the growing content of ash, were observed also in batches containing diverse kinds of biomass ashes, but linked to different phenomenological processes. SEM micrographs of bodies containing sugarcane bagasse ash [16, 22] revealed an increasing in closed pores explained by the combustion of the organic fraction of the ashes. TG curve indicates that ash-bearing batch had significant mass loss (LOI ~12wt%), mostly matching the exothermic event around 580°C related to the decomposition and oxidation of organic compounds (charcoal and organic matter), with the release of CO_2 [22]. Otherwise, the increasing in porosity recorded for batches containing coffee husk ash, could be related to the decomposition of calcium carbonate, which occurs with significant weight loss (~20wt%) associated with a strong endothermic event, between 825 and 1090°C [30]. The behaviour of bodies which incorporate rice straw ash [14,29], is much more similar to that of the batches studied here. In fact, they are

characterized by a significantly lower LOI with respect to both sugarcane bagasse ash and coffee husk ash (Table 1). In this case, the gas development might be due to the high content of gas-generating substances such as Cl for rice straw ash and calcite and Fe_2O_3 for BBA, which, in combination with the narrow vitrification range, led to swelling of the body.

The intensification of this phenomenon can be observed in our samples passing to 1220°C (Figure 14). At this temperature it appears clear how the technological properties are affected by the microstructure, which took the traits of the over-firing. Indeed, the inversion of shrinkage trend and the significant loss of bulk density for the waste-bearing batches (Figures 6-7) are mirrored in SEM micrographs by a pore coarsening effect. Large pores, with a diameter up to 60 µm, clearly testify the occurrence of de-sintering processes related to bloating phenomena, which can foster pyroplastic deformations. On the other hand, the benchmark C0 exhibits a good stability at the highest temperature with respect to the other batches, as also testified by the HSM stability test (Figure 8), even if an incipient pore coarsening can be appreciated.

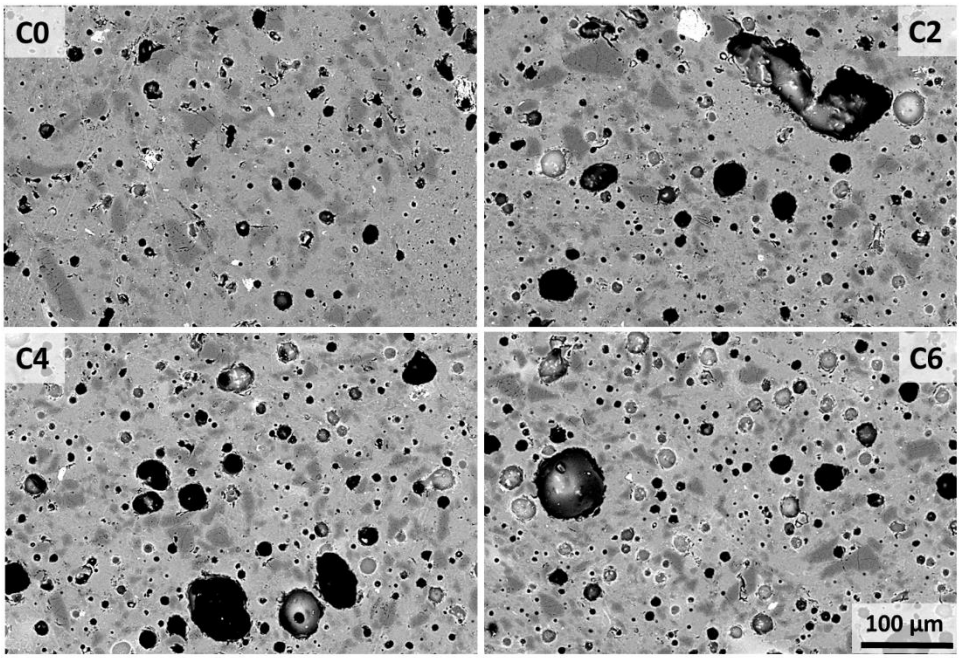

Figure 14. SEM-BS micrographs of all bodies fired at 1220°C (scale bar = 100 µm).

4. CONCLUSIONS

This study investigated the feasibility of biomass bottom ash recycling in porcelain stoneware bodies, offering a comprehensive analytical approach from the technological, mineralogical and microstructural point of views. Due to its physical-chemical properties, the BBA was introduced in the ceramic batch in partial substitution of feldspars, up to 6wt%. The simulation of all the industrial tile manufacturing process allowed to highlight for the first time a bottleneck related to the rheological

behavior of the slips. The presence of ashes, in fact, induced a considerable increase in the viscosity of the slip during the wet milling, which was overcome by a slight addition of deflocculant, for a total of 0.6wt% on the dry mass. This hindrance was not pointed out in previous studies, since the ashes are usually added by dry route to the ceramic batches. This work demonstrated that this obstacle present in the wet milling process, typically used in the industrial practice, can be easily managed.

There were no further technological drawbacks in the process simulation. Moreover, no significant variations with respect to technological parameters, such as particle size distribution, springback, green and dry bulk density were identified, indicating that the introduction of ash, within certain limits, guarantees the maintenance of the required properties of the semi-finished products along the production line. As far it concerns the firing behavior, the introduction of ash allowed to lower the firing temperature by 20°C (1180°C) with respect to the waste-free batch (1200°C), while maintaining good levels of densification, with bulk density around 2.4 g/cm^3. However, it was noticed a tendency of the waste-bearing batches to instability at high temperatures, so that the gresification window tends to be rather narrow. As known, in fact, the power in reducing the temperature of maximum densification assigns to the biomass ashes the role of fluxing agents, but their increasing amount in the ceramic batches can cause a fast decrease in bulk density. In this sense, it is important to identify the exact firing temperature of the bodies, in order not to incur phenomena related to the over-firing of ceramic products, such as bloating, as suggested by SEM and HSM results.

The study of the phase evolution at different firing temperatures, permitted to unveil different behaviors. The introduction of ash led to a delay in feldspars melting of about 100°C compared to the reference sample; at the same time, already at 1000°C, the glassy phase appears to be higher in the samples with ash, probably because BBA induced melting reactions at lower temperature with respect to the feldspars. Moreover, the presence of bottom ash led to persistence of more feldspars at the end of firing with respect to the waste-free body. This is thought to occur since ash melt in place of the feldspars, leaving a larger amount of these minerals at the end of the process. Even if, as far as we know, no quantitive data of the mineralogical composition of ashes-bearing bodies are available, a similar behaviour, with the waste melting in place of feldspars, was already osebrved for glassy wastes and alternative strong fluxes.

The addition of ash to the batches, in partial replacement of the classical fluxes, speeded up the sintering process, leading to the early formation of the amorphous phase and the decreasing of the maximum temperature of densification. Effects of this "anticipation" can also be read in the SEM images. The micrographs revealed how phase evolution coincides with the microstructure evolution, so samples show different textural characteristics at the same temperature, coinciding with different sintering stage.

Taking into account all the collected data, the ceramic product obtained from the batch containing 4wt% of bottom ash is the best choice among the tested ones, showing values perfectly matching the standard requirements for porcelain stoneware. In contrast, the 6wt% replacement represents the limit of introduction for this type of formulation. The results obtained are therefore promising from an industrial point of view, and demonstrate for the first time the feasibility of biomass bottom ash recycling in porcelain stoneware bodies along all the production line, with small variation just in the step of the wet milling.

ACKNOWLEDGEMENTS

This work was undertaken within the CNR project "*Capitale naturale e risorse per il futuro dell'Italia (FOE 2020)*" as deliverable "*Utilizzo razionale di risorse tramite riduzione di materia prime critiche, valorizzazione degli scarti e riciclo efficace*" (Dipartimento di Scienze Chimiche e Tecnologie dei Materiali – DSCTM). *CUP=B85F21002120005*

REFERENCES

[1] Baraldi, L. (2019). World production and consumption of ceramic tiles. Ceramic World Review, 133, 48–63.

[2] Dondi, M., García-Ten, J., Rambaldi, E., Zanelli, C., Vicent-Cabedo, M. (2021). Resource efficiency versus market trends in the ceramic tile industry: Effect on the supply chain in Italy and Spain. Resources, Conservation and Recycling, 168, 105271.

[3] Palmonari, C., Timellini, G. (2000). Environmental impact of the ceramic tile industry. New approaches to the management in Europe. Ceramica Acta 12 (4), 16–35.

[4] Blengini, G.A., Shields, D.J. (2010). Green labels and sustainability reporting: Overview of the building products supply chain in Italy. Management of Environmental Quality: An International Journal 21 (4), 477–493.

[5] Gabaldón-Estevan, D., Criado, E., Monfort, E. (2014). The green factor in European manufacturing: a case study of the Spanish ceramic tile industry. Journal of Cleaner Production 70, 242–250.

[6] WGBC (2022). World Green Building Council. https://www.worldgbc.org/ [last accessed on January 26, 2022].

[7] ISO 17889 (2021). Ceramic tiling systems — Sustainability for ceramic tiles and installation materials — Part 1: Specification for ceramic tiles. International Organization for Standardization.

[8] Andreola, N.M.F., Barbieri, L., Lancellotti, I., Leonelli, C., Manfredini, T. (2016). Recycling of industrial wastes in ceramic manufacturing: State of art and glass case studies. Ceramics International 42 (12), 13333–13338.

[9] Coronado, M., Blanco, T., Quijorna, N., Alonso-Santurde, R., Andrés, A. (2015). Types of waste, properties and durability of toxic waste-based fired masonry bricks. Eco- Efficient Masonry Bricks and Blocks. Woodhead Publishing, 129–188.
[10] Coronado, M., Segadães, A.M., Andrés, A. (2015). Using mixture design of experiments to assess the environmental impact of clay-based structural ceramics containing foundry wastes. Journal of Hazardous Materials 299, 529–539.
[11] Cifrian, E., Coronado, M., Quijorna, N., Alonso-Santurde, R., Andrés, A. (2019). Waelz slag-based construction ceramics: effect of the trial scale on technological and environmental properties. Journal of Material Cycles and Waste Management, 21 (6), 1437–1448.
[12] Zanelli, C., Conte, S., Molinari, C., Soldati, R., Dondi, M. (2021). Waste recycling in ceramic tiles: a technological outlook. Resources, Conservation & Recycling 168, 105289.
[13] Guzman, A., Torres, J., Cedeno, M., Delvasto, S., Borras, V.A., Vilches E.J.S. (2013). Fabricacion de gres porcelanico empleando ceniza de tamo de arroz en sustitucion del feldespato. Boletín de la Sociedad Espãnola de Ceramica y Vidrio 52 (6), 283–290.
[14] Guzman, A., Delvasto, A., Francisca Quereda, V. M., Sanchez, V. (2015). Valorization of rice straw waste: production of porcelain tiles. Ceramica 61 (360), 442–449.
[15] Amutha, K., Sivakumar, G., Elumalai, R. (2014). Comparison studies of quartz and biosilica influence on the porcelain tiles. International Journal of Scientific and Engineering Research 5 (3), 102–105.
[16] Schettino, M.A., Holanda, J.N. (2015). Processing of porcelain stoneware tile using sugarcane bagasse ash waste. Processing and Application of Ceramics 9 (1), 17–22.
[17] Abeid, S., Park, S.E. (2018). Suitability of vermiculite and rice husk ash as raw materials for production of ceramic tiles. International Journal of Materials Science and Applications 7 (2), 39.
[18] Olokode, O.S., Aiyedun, P.O., Kuye, S.I., Anyanwu, B.U., Eng, B., Owoeye, F.T., Adekoya, T.A. (2013). Optimization of the quantity of wood ash addition on kaolinitic clay performance in porcelain stoneware tiles. Pacific Journal of Science and Technology 14 (1), 48–56.
[19] Paranhos, R.J.S., Acchar, W., Silva, V.M. (2017). Use of sugarcane bagasse ashes as raw material in the replacement of fluxes for applications on porcelain tile. Materials Science Forum 881, 383–386.
[20] Fernandes, H.R., Ferreira, J.M.F. (2007). Recycling of chromium-rich leather ashes in porcelain tiles production. Journal of the European Ceramic Society 27 (16), 4657–4663.
[21] Andreola, N.M.F., Martín, M.I., Ferrari, A.M., Lancellotti, I., Bondioli, F., Rincon, J.M., Romero, M., Barbieri, L. (2013). Technological properties of glass-ceramic tiles obtained using rice husk ash as silica precursor. Ceramics International 39 (5), 5427–5435.

[22] Faria, K.C.P., Holanda, J.N.F. (2016). Thermal behavior of ceramic wall tile pastes bearing solid wastes. Journal of Thermal Analysis and Calorimetry 123 (2), 1119–1127.
[23] Jamo, H.U., Noh, M.Z., Ahmad, Z.A. (2015). Effects of mould pressure and substitution of quartz by palm oil fuel ash on compressive strength of porcelain. Advanced Materials Research 1087, 121–125.
[24] Barbieri, L., Corradi, A, Lancellotti, I., Manfredini, T. (2002). Use of municipal incinerator bottom ash as sintering promoter in industrial ceramics. Waste Management, 22, 859–863.
[25] Bourtsalas, A., Vandeperre, L.J., Grimes, S.M., Themelis, N., Cheeseman, C.R. (2015). Production of pyroxene ceramics from the fine fraction of incinerator bottom ash. Waste Management, 45, 217- 225.
[26] Dana, K., Dey, J., Das, S.K. (2005). Synergistic effect of fly ash and blast furnace slag on the mechanical strength of traditional porcelain tiles. Ceramics international 31 (1), 147–152.
[27] Wang, H., Zhu, M., Sun, Y., Ji, R., Liu, L., Wang, X. (2017). Synthesis of a ceramic tile base based on high-alumina fly ash. Construction and Building Materials 155, 930–938.
[28] Dana, K., Das, S.K. (2002). Some studies on ceramic body compositions for wall and floor tiles. Transactions of the Indian Ceramic Society 61 (2), 83–86.
[29] Guzmán, Á., Gordillo, S.M., Delvasto, A.S., Quereda, V.M.F., Sánchez, V.E. (2016). Optimization of the technological properties of porcelain tile bodies containing rice straw ash using the design of experiments methodology. Ceramics International, 42(14), 15383- 15396.
[30] Acchar, W., Dultra, E.J.V., Segadães, A.M. (2013). Untreated coffee husk ashes used as flux in ceramic tiles. Applied Clay Science 75-76, 141–147.
[31] Acchar, W., Avelino, K.A., Segadães, A.M. (2016). Granite waste and coffee husk ash synergistic effect on clay-based ceramics. Advances in Applied Ceramics 115 (4), 236–242.
[32] Acchar, W., Dultra, E.J. (2015). Porcelain tile. Ceramic Materials from Coffee Bagasse Ash Waste. Springer International Publishing, 3–15.
[33] Carvalho, V.H.M., Rocha, M.B.S., Dultra, E.J.V., Acchar, W., Segadães, A.M. (2017). Beneficiation of coffee husk ashes to be used as flux in porcelain tiles. Proceedings 4th WASTES: Solutions, Treatments and Opportunities, September 25-26, 2017, Guimarães, Portugal, 2-4.
[34] Sivakumar, G., Hariharan, V., Shanmugam, M., Mohanraj, K. (2014). Fabrication and properties of bagasse ash blended ceramic tiles. International Journal of ChemTech Research, 6(12), 4991-4994.
[35] Noh, M.Z., Jamo, H.U., Ahmad, Z.A. (2014). Effect of temperature and composition of palm oil fuel ash on compressive strength of porcelain. Applied Mechanics and Materials, 660, 173-177.

[36] Aripin, A., Tani, S., Mitsudo, S., Saito, T., Idehara, T. (2010). Fabrication of unglazed ceramic tile using dense structured sago waste and clay composite. Indonesian Journal of Materials Science 11 (2), 79–82.

[37] Novais, R.M., Seabra, M.P., Labrincha, J.A. (2015). Wood waste incorporation for lightweight porcelain stoneware tiles with tailored thermal conductivity. Journal of Cleaner Production 90, 66–72.

[38] Naga, S.M., Awaad, M., El-Mehalawy, N., Antonious, M.S. (2014). Recycling of fish bone ash in the preparation of stoneware tiles. International Ceramic Review 63 (1-2), 15–18.

[39] Awaad, M., Naga, S.M., El-Mehalawy, N. (2015). Effect of replacing weathered feldspar for potash feldspar in the production of stoneware tiles containing fish bone ash. Ceramics International 41 (6), 7816–7822.

[40] European waste catalog, directive 75/442/EEC. ICER INTERNATIONAL. Research and Innovation Portal and of the circular economy https://www.icer-grp.com/index.php/en/services/tecnopedia-en/information-on-ewc-codes [last accessed on January 26, 2022].

[41] Gualtieri, A. F., Mazzucato, E., Venturelli, P., Viani, A., Zannini, P., Petras, L. (1999). X-ray Powder Diffraction Quantitative Analysis Performed in Situ at High Temperature: Application to the Determination of NiO in Ceramic Pigments. Journal of Applied Crystallography, 32, 808-813.

[42] Larson, A.C., Von Dreele, R.B. (1994). General structure analysis system "GSAS". Los Alamos National Laboratory Report, Los Alamos, LAUR 86−748.

[43] Toby, B.H. (2001). EXPGUI, A graphical user interface for GSAS. Journal of Applied Crystallography, 34, 210−213.

[44] Modolo, R.C.E., Tarelho, L.A.C., Teixeira, E.R., Ferreira, V.M., Labrincha, J.A. (2014). Treatment and use of bottom bed waste in biomass fluidized bed combustors. Fuel Processing Technology 125, 170-181.

[45] Cabrera, M., Galvin, A.P., Agrela, F., Carvajal, M.D., Ayuso, J. (2014). Characterisation and technical feasibility of using biomass bottom ash for civil infrastructures. Construction and Building Materials, 58, 234-244.

[46] Khan, A., Jong, W., Jansens, P., Spliethoff, H. (2009). Biomass combustion in fluidized bed boilers: Potential problems and remedies. Fuel Processing Technology 90, 21–50.

[47] Hinojosa, M.J.R., Galvın, A.P., Agrela, F., Perianes, M., Barbudo, A. (2014). Potential use of biomass bottom ash as alternative construction material: conflictive chemical parameters according to technical regulations. Fuel 128, 248-259.

[48] Sklivaniti, V., Tsakiridis, P.E., Katsiotis, N.S., Velissariou, D., Pistofidis, N., Papageorgiou, D. (2017). Valorisation of woody biomass bottom ash in Portland cement: a characterization and hydration study. Journal of Environmental Chemical Engineering. 5 (1), 205-213.
[49] Vassilev, S.V., Baxter, D., Andersen, L.K., Vassileva, C.G. (2013). An overview of the composition and application of biomass ash. Part 1. Phase-mineral and chemical composition and classification. Fuel 105, 40-76.
[50] Nurmesniemi, H., Manskinen, K., Pöykiö, R, Dahl, O. (2012). Fertilizer properties of the bottom ash and fly ash from a large-sized (115 mw) industrial power plant incinerating wood-based biomass residues. Journal of the University of Chemical Technology and Metallurgy, 47, 1, 43-52.
[51] Dondi, M., Guarini, G., Conte, S., Molinari, C., Soldati, R., Zanelli, C. (2019). Deposits, composition and technological behavior of fluxes for ceramic tiles. Periodico di Mineralogia, 88, 235-257.
[52] Zanelli, C., Domínguez, E., Iglesias, C., Conte, S., Molinari, C., Soldati, R., Guarini, G., Dondi, M. (2019). Recycling of residual boron muds into ceramic tiles. Boletín de la Sociedad Española de Cerâmica y Vidrio 58 (5), 199–210.
[53] Sánchez, E., Garcia-Ten, J., Sanz, V., Moreno, A. (2010). Porcelain tile: Almost 30 years of steady scientific-technological evolution. Ceramics International, 36, 831–45.
[54] Conte, S., Zanelli, C., Ardit, M., Cruciani, G., Dondi, M. (2020). Phase evolution during reactive sintering by viscous flow: Disclosing the inner workings in porcelain stoneware firing. Journal of the European Ceramic Society, 40, 1738–1752.
[55] Devineau, K., Pichavant, M., Villiéras, F. (2005). Melting kinetics of granitic powder aggregates at 1175 C°, 1 atm. European Journal of Mineralogy, 17, 387–398.
[56] Conte, S., Zanelli, C., Molinari, C., Guarini, G., Dondi, M. (2020). Glassy wastes as feldspar substitutes in porcelain stoneware tiles: Thermal behaviour and effect on sintering process. Materials Chemistry and Physics, 256, 123613.
[57] Tavares Brasileiro, C., Conte, S., Contartesi, F., Gomes Melchiades, F., Zanelli, C., Dondi, M., Ortega Boschi, A. (2021). Effect of strong mineral fluxes on sintering of porcelain stoneware tiles. Journal of the European Ceramic Society, 41, 5755–5767.
[58] Zanelli, C., Raimondo, M., Dondi, M., Guarini, G., Tenorio, P. (2004). Sintering mechanisms of porcelain stoneware tiles. Proceedings Qualicer 2004, 247-259.

Recycling of bottom ash from biomass combustion in porcelain stoneware tiles: effects on technological properties, phase evolution and microstructure

Sonia Conte[1*], Daniele Buonamico[2], Tommaso Magni[2], Rossella Arletti[2], Michele Dondi[1], Guia Guarini[1], Chiara Zanelli[1]

[1]CNR-ISTEC, National Research Council, Institute of Science and Technology for Ceramics, Via Granarolo, 64-48018, Faenza, Italy

[2]Department of Chemical and Geological Science, University of Modena and Reggio Emilia, Via Giuseppe Campi, 103-41125 Modena, Italy

ABSTRACT

This work aims to evaluate the use of bottom biomass ash as an alternative raw material in porcelain stoneware bodies. For this purpose, ash coming from a biomass thermoelectric power plant in Emilia-Romagna (Italy) was selected and its chemical, mineralogical and thermal properties determined. Data indicated its technological role as a flux, so it was introduced in a porcelain stoneware batch in partial replacement of feldspars and experimented at laboratory scale. A bottleneck, relative to the rheological behavior of the slips, was overcome by a slight deflocculant increase. The powder compacts were fired from 1000 to 1220°C in order to follow the evolution of the technological properties, phase composition (XRPD-Rietveld) and microstructure (SEM). The introduction of ash allowed to lower the firing temperature by 20°C, while keeping the technological properties comparable with those of the benchmark. Moreover, the mineralogical and microstructural data revealed different sintering kinetics.

Keywords: bottom ash, microstructure, porcelain stoneware, technological properties, waste recycling.

***Corresponding author**: Sonia Conte

mail: sonia.conte@istec.cnr.it,

permanent address: Via Granarolo, 64, 48018 Faenza RA, Italy

phone: +390546699711

fax: +39054669979

1. INTRODUCTION

The manufacture of ceramic tiles is globally steady, with a production around 13 billion square meters in the latest years [1], implying a constant demand for raw materials attaining an estimated global consumption beyond 300 million tons per year [2]. On the other hand, the progressive depletion of the main mineral deposits that this production rate imposes, is forcing the ceramic industry to look for suitable substitutes, which guarantee specific technological properties to the finished product. The efforts of the ceramic industry in the latest years to replace natural raw materials with secondary ones, was also driven by marketing reasons supported through green certificates [3-5], like Ecolabel and the LEED credits (The Leadership in Energy and Environmental Design; WGBC, 2022 [6]), and the standard on the sustainability of ceramic tiles (ISO 17889, 2021 [7]). To make the production completely sustainable in the long run, in view of the transition to a circular economy, but ensuring the high technological performances of the product, represents a challenge for the ceramic industry [8]. Although to date this industry has proven to be able to recycle its own processing residues very efficiently, the use of waste from other sources is currently rather limited. Among the materials that could be tested as secondary raw material in ceramic production, biomass combustion ashes represent an opportunity, since biomass is increasingly replacing fossil fuel in thermal power plants and, for this reasons, ashes are locally available in significant amount.

In principle, silicate ceramics are good waste acceptors since they are composed of heterogeneous bodies: a mixture of various minerals that undergo phase transformations during processing, especially at the firing stage. This is favorable for the waste incorporation because a highly heterogeneous mix is intrinsically prone to accommodating extraneous components. At any rate, a certain waste is increasingly tolerated as far as its technological behavior resembles those of conventional raw materials [9-12].

Nowadays, what is lacking to promote the widespread recourse to recycled raw materials is the knowledge about the effect of a specific waste in ceramic tile manufacturing. In this context, a recent work of Zanelli and co-workers [12] overviewed the effect of waste recycling on technological behavior and technical performance of ceramic tiles. Such a technological outlook regarding bottom ashes from biomass combustion revealed that there is little information about the technological behavior during the pre-firing processes (from body preparation to pressing and drying) while the firing step has been more investigated [13-23]. Despite the almost absence of studies on the pre-firing steps, it emerges that they are the more critical, due to the high susceptibility of the ash to moisture (tendency to cementation), which can cause several problems in the storage and handling of this waste [12].

In general, bottom ashes from biomasses are the product of a combustion by thermal power plants to produce energy by burning organic matter. Combustion processes give rise to residues that can be basically distinguished between a quantitatively predominant coarse-grained bottom ash [24-25] and fly ash that generally has a very fine particle size [26-27]. Combustion of biomasses produces different ashes, since sources can be extremely varied: rice husk [14,17,21,28-29], coffee husk [30-33], sugar cane bagasse [16,19,22,34], palm oil and sago [23,35-36], cereal straw and stalk [13,15], wood and forestry wastes [18,37], fish bone [38-39] and leather waste [20]. Biomass ashes exhibit therefore a considerably variable composition, primarily depending on the source (Table 1). In general, plant-based ashes are siliceous materials, poor in alumina and rich in P_2O_5 with respect to ceramic bodies, while the content in alkalis and alkali-earths is rather high, especially some ashes peak over 20% CaO or over 10% K_2O (Tables 1 and S1, supplementary material).

Table 1.

Laboratory experimental data relative to the firing behavior and technical performance of ceramic tiles containing different kind of biomass ashes, indicated that they seem generally adequate to replace fluxes or fillers in low proportion (≤10wt%) in porcelain stoneware. A significant reduction of firing temperature is reported, without influencing too much the technical properties and the tile microstructure. This occurred with ashes from coffee husk, rice straw, and sugarcane bagasse, which are characterized by high alkali values [13-14,16,19,30,32]. Positive results were registered also with other wastes, like palm oil ash, as a substitute of quartz in a porcelain batch, which led to an increase in compressive strength [23]. Essentially, there are evidences that these wastes play as a strong flux, reducing the temperature of maximum densification, in accord with a composition rich in Fe, Na, K and poor in Si and Al. A darker colour after firing and a fast decrease in bulk density were observed for increasing ash amount [12-14,17]. The literature agrees that the use of biomass ash can lead to properties matching the standards for porcelain stoneware tiles, with a recommended recyclable amount in most cases between 5 and 10%. Anyway, to date, the technological feasibility of ashes recycling can be affirmed only in relation to the firing behaviour. In fact, the technical constraints of the pre-kiln processes have not been adequately assessed and there may be technological pitfalls. Moreover, detailed information unravelling the effect of the substitution on the phase and microstructure transformations occurring at the different stages of the firing are not available. This is a crucial point in understanding the reasons of eventual changes during sintering.

The goal of this work is therefore to evaluate the technological feasibility of the biomass ash recycling in porcelain stoneware bodies, in relation to all the industrial steps of the ceramic tiles production (milling – granulation – shaping – drying – firing), in order to identify possible bottlenecks along the

manufacturing line. This was possible by simulating the industrial cycle at the laboratory scale, verifying the effect of the ash introduction not only on the fired products but also on the semi-finished ones. In addition, a detailed characterization of the phase composition and microstructure of the fired bodies at different temperatures was carried out to understand the way by which the biomass ash affects the viscous sintering.

2. EXPERIMENTAL

In the present work bottom ash from biomass combustion (BBA), coming from a thermoelectric power plant in Faenza, Emilia-Romagna (Italy), was exploited as an alternative raw material in porcelain stoneware bodies. These bottom ashes represent the combustion product of woody material, grass, pomace and a mix of tree essences, treated at a declared combustion temperature between 700 and 1000°C. They are classified by the CER code (European waste catalog, directive 75/442/EEC) CER 10 01 01: Waste produced by thermal power plants and other thermal plants, defined as non-hazardous materials [40]. Bottom ashes are, by definition, coarse-grained, so their particle size distribution was determined by sieving test (sieves sequence 4, 2, 1, 0.5, 0.25, 0.125, 0.063 mm). Moreover, the ash was characterized from the chemical, mineralogical, and thermal point of view. The chemical composition was determined by XRF-WDS (PW 1480, Philips) and reported in Table 1, while the mineralogical composition by XRPD analysis (X'PERT PRO, PANalytical). The thermal behavior of the ash was studied by thermogravimetric analysis (TGA-DTG) ~~and differential thermal (DTA)~~ performed under flowing air on powder (~15 mg) up to 1050°C, using a TG/DTA 320U thermobalance and 20°C/min heating rate, alumina crucibles and Pt–Pt10Rh thermocouples. The fusibility was determined by hot stage microscopy (HSM Misura 3- 402ES/3, Expert System Solution) with a cycle of 10°C/min up to 1600°C. The results indicated a technological role of BBA as a fluxing component in substitution of feldspars. Therefore, four different porcelain stoneware batches were designed: a benchmark without ash named C0 and three bodies with increasing BBA amount up to 6wt%, named C2-C4-C6 (Table 2). The maximum amount of ash (6wt%) was decided on the basis of literature results [12-23] and experimental tests. Indeed, preliminary laboratory tests indicated that the introduction of this ash brings about a worsening of rheological behavior of the slips (increase of viscosity measured by the time of flow through Ford cup). This bottleneck can be easily managed in batches containing ash up to 6wt% by a deflocculant increase (0.6wt% instead of 0.3wt%). On the other hand, a higher amount of ash would entail an excessive deviation from the technological behavior of conventional raw materials.

Table 2.

The four designed batches were experimented at the laboratory scale, simulating the industrial tile-making process. Before adding it to the batches, the ash was ground using a hammer mill with a 500 μm grid. Then all the raw materials were ball milled in a porcelain jar using dense alumina grinding media, 40% water (by weight of the slip) and 0.6% deflocculant (sodium tripolyphosphate) by weight of dry batch, for 20 minutes. The slips were oven dried, de-agglomerated (hammer mill with grid of 500 μm) and manually granulated (sieve 2 mm, moisture ~8wt%). Powders were compacted with a hydraulic press (40 MPa) into 110×55×5 mm tiles, dried in an electric oven at 105 ± 5°C overnight and characterized for: particle size distribution (ASTM C958), springback (i.e., $100(L_p-L_m)/L_m$, where L_p is the length of the pressed tile and L_m is the length of the mold), green and dry bulk density (weight/volume ratio), as reported in Table 3.

Powder compacts were fast fired in an electric roller kiln (ER15; Nannetti, Faenza, Italy) at seven different maximum temperature ranging from 1000 to 1220°C (T_{max}: 1000, 1100, 1130, 1160, 1180, 1200, 1220°C), with a thermal cycle of about 60 min cold-to-cold and 5 min of dwell time at T_{max}. Technological properties, determined after firing the specimens at the different T_{max}, are: linear firing shrinkage (i.e., $100(L_m-L_f)/L_m$ where L_f is the length of the fired tiles and L_m is the length of the mold), water absorption, bulk density and open porosity (ASTM C373) (Table S2, supplementary material). CIE ‐ Lab colorimetry (ISO 10545 ‐ 16, MSXP ‐ 4000; Hunterlab, Reston, VA, USA) of sintered tiles was also performed and the L^*, a^*, and b^* values reported in Table S3 (supplementary material).

The sintering behavior of the four batches was investigated by in-situ experiments on specimens (approximately 5x5x5 mm) cut from the pressed compacts. Experiments were carried out by optical thermo-dilatometry (TA, ODP868, Germany) with a firing schedule consisting of heating ramp (40°C/min) up to 1180°C and testing the body stability by increasing temperature by steps of 10°C up to 1220°C (with 5 min dwell time at every step).

X-Ray powder diffraction patterns were collected on powdered fired tiles after the addition of 10wt% of Al_2O_3 standard. The samples were laterally loaded on an Al-sample holder and the patterns were collected using a X'PERT PRO, PANalytical with θ-θ geometry and CuKα radiation, in the 0–110°2θ range, with counting times of 120 seconds for each step. The combined RIR-Rietveld method, which enables the quantitative phase analysis (QPA) and the calculation of both the crystalline and amorphous fractions [41] was performed by using the GSAS software [42] with the EXPGUI interface [43]. The results and details of the refinements are reported in Table S4 (supplementary material).

The microstructural evolution of the four batches fired at temperatures corresponding to specific stage of the sintering process (start, intermediate stage, maximum densification and overfiring) was

observed by scanning electron microscopy (JSM-6010 LA InTouchScope, graphite sputtered polished surface, JEOL, USA).

3. RESULTS AND DISCUSSION

3.1. Characterization of biomass bottom ash

The grain size curve of the biomass bottom ash is shown in Figure 1, by which a d_{50} of 2.05 mm can be derived. Such a grain size distribution is slightly coarser than those observed for wood biomass ashes by Modolo and co-workers [44] and Cabrera and co-workers [45], which appear, on average, finer. Moreover, the maximum diameters of the particles exceed the size of 4 mm, in line with the literature studies cited above.

Figure 1.

From the chemical point of view, the BBA are generally mainly composed by Si, Ca, Al, Fe, Mg, K and P [46], even if the relative concentration of a specific element is function of the biomass from which the ashes originated (Table 1). The BBA object of this study shows a chemical composition quite compatible with those relative to ashes coming from the combustion of agricultural and forest residues and from a mix of them [18,44,47-48]. Compared to the fluxes it has replaced, the bottom ash shows peculiar features, with a lower content of SiO_2 and Al_2O_3 (~43 and ~9%wt, respectively) and higher amount of CaO, Fe_2O_3, MgO and P_2O_5 (Table S1).

The qualitative XRPD analysis of BBA indicates the presence of quartz, K-feldspar, leucite, wollastonite, cristobalite, melilite, calcite and portlandite (Figure 2), also in this case mostly matching the literature data relative to biomass bottom ashes [49-50].

Figure 2.

The behavior of the BBA as a function of temperature was evaluated through the combination of thermogravimetric analysis (TG-DTG) ~~and differential thermal (DTA)~~ and by hot-stage microscopy (HSM). As shown in Figure 3, the weight loss of the ash is about 3wt%, mirroring the value obtained as loss on ignition (Table 1). It occurs mainly in two steps, both associated to very weak endothermal reactions. The first is between 300 and 500°C (~0.5%, DTG peak at ~480°C), and the second is between 550 and 770°C (~2.5%, DTG peak at ~750°C). The former can be attributed to thermal decomposition of portlandite and the latter to calcite.

Figure 3.

The fusibility degree of the BBA is demonstrated by the softening and melting temperatures, as obtained by HSM, which are close to 1210 and 1240°C, respectively. Such characteristic temperatures can be compared with those of various ceramic fluxes through the fusibility chart reported in Figure 4, which depicts the fields of fusibility from very low to very high and a zone of high risk of bloating (related to higher contents of iron oxide) [51]. The BBA is characterized by a very high fusibility and a low risk of bloating.

Figure 4.

It should be remembered that the chemical and mineralogical composition, as well as the thermal behavior, of biomass bottom ashes is extremely variable, depending not only on the biomass of origin but also on the processes with which were generated. The characterizations of the ashes themselves before their employ are therefore of fundamental importance. On the other hand, these ashes are classified by the CER code (European waste catalog, directive 75/442/EEC) as non-hazardous materials, and, in force of this and their properties, they represent an excellent candidate for in-depth technological investigations.

3.2. Technological properties of semi-finished and finished porcelain stoneware tiles

The BBA had a significant impact in the first step of production, i.e., the wet milling. The ash led to a worsening of the rheological properties of the slip with a relevant increase in viscosity. Anyway, this bottleneck was easily overcome thanks to a slight addition of deflocculant (from 0.3 to 0.6wt%). This correction allowed an adequate wet milling, obtaining bodies with very similar particle size distribution, with a median particle diameter between 3.3 and 3.9 μm (Table 3 and Figure 5), that matches usual values in ceramic tile production.

Table 3.

Figure 5.

The presence of the ash did not modify the technological behavior of porcelain stoneware bodies during the granulation, shaping and drying steps. Small variations were observed also for the technological properties of semi-finished products (Table 3). Specifically, a slight increase in both green and dry bulk density in bodies containing ash implies an improvement in the degree of compaction due to the presence of BBA. On the other hand, the springback, even if slightly decreased, is still in the range usually accepted in the industrial practice, i.e., 0.3–0.6 cm/m [52].

Technological properties determined after firing at different maximum temperatures are reported in Figures 6-7 and Table S2, supplementary materials.

Figure 6.

At variance with the semi-finished products, the BBA significantly influenced the firing behavior. The linear shrinkage decreased with the amount of ash (Figure 6). Actually, increasing BBA from 2 to 6%wt led to a progressive reduction of linear shrinkage values, less pronounced for batch C2. Moreover, the waste-bearing bodies reached their maximum shrinkage at 1180°C, showing similar values among them and also close to the benchmark. Beyond this temperature, they exhibit an expansion of the ceramic bodies, while the waste-free body C0 continued to shrink up to 1200°C, reaching the highest value of the set (5.56 cm/m), and remained stable even at 1220°C.

Taking into account water absorption and bulk density, it is possible to observe their evolution over a wide range of temperatures (Figure 7 and Table S2). At 1000°C, the batches containing ash are characterized by a slightly higher bulk density with respect to the benchmark, corresponding to a lower water absorption, likely inherited from the higher bulk density of unfired compacts (Table 3). At 1100°C, it is no longer possible to observe a clear distinction in behavior between the waste-bearing batches and the reference, mostly because of the sample C6, characterized by a delay in densification in the 1100-1130°C range, with respect to batches C2 and C4. Starting from 1100°C onwards there is, for all the samples, a change in the slope of the curves with a significant increase in density and a corresponding decrease in water absorption, indicating an increase in sintering kinetics.

Figure 7.

At 1180°C the batches with BBA reached their maximum density, with values very similar for C2 and C4, slightly lower for C6; at this same temperature they also show values of water absorption ≤0.5%, which allow to define 1180°C as their adequate firing temperature. The decreasing of the maximum bulk density with increasing amount of ashes has been observed also with the introduction of rice straw and rice husk ashes [14,17], bagasse ashes [16] and coffee husk ashes [30]. Even if at 1200°C the water absorption is lower for C2-4-6 bodies, they suffer from a significant loss of density, which, in accordance with the linear shrinkage data, indicates an expansion of the ceramic body, more accentuated at 1220°C. On the other hand, for the benchmark the sintering process is still going on at 1180°C, as witnessed by the high water absorption (2.6%) and still increasing bulk density values. Indeed, for this batch the densification is accomplished at 1200°C, i.e., 20°C higher than samples containing ash. Nevertheless, it is worth noting that C0 is characterized by a more pronounced stability even at the highest temperature with respect to the other batches. Indeed, in Figure 8, it is possible to notice that the C0 remained stable once reached the maximum densification, still going on to densify up to at 1220°C, where a hint of instability can be glimpsed. Otherwise, for the bodies with ash, once reached the maximum densification there is a rapid expansion of the specimens

(inferred from the inversion of the curves, that indicates an increase in volume), related to de-sintering processes. These bloating phenomena, corroborated by the decrease in shrinkage, bulk density and increase in closed porosity (Table 3 and SEM micrographs), were observed also in porcelain tiles containing rice straw ashes [14,29], especially when present in high amount (i.e., 60wt%), and are generally caused by the greater content in gas-releasing substances (Fe_2O_3, chlorides, also as LOI) coming from the ash.

Figure 8.

For as concerns the colour of the tiles (Table S3, supplementary materials), considering those fired at the maximum densification temperature (1180°C for C2-4-6 and 1200°C for C0), the presence of ash induced very small variations. The main changes concern the L^* parameter: all the ash-bearing bodies turned a bit darker (from 73 of the benchmark down to 67 L^*). At the same time, they exhibit slightly higher values of a^* so resulting a little redder, and, just in the case of C6, slightly higher values of also b^*, resulting yellower than body C0. These colour changes can be related with the variation of iron content, since the ash introduction implies a little increase in the total iron amount of the batches (Table 2).

3.3 Phase composition of fired porcelain stoneware tiles

Porcelain stoneware is typically composed of quartz and feldspar remnants, and neo-formed mullite, embedded in an abundant vitreous phase [53-54]. The phase composition of the four bodies fired at the seven different temperatures (28 samples) are summarized in Figure 9 and reported in Table S4 (supplementary material).

The presence of quartz decreases as a function of the increasing temperature in all the batches, indicating its partial melting, with a rather steady rate over 1100°C. This general tendency is expected, since it is known that quartz dissolution has an exponential dependence on firing temperature [55]. In the ash-free C0, the quartz dissolution rate increases later with respect to the ash bearing samples and quartz remained in a slightly higher amount at the end of the ramp. More in detail, the fast dissolution of quartz in C0 started from 1130°C with a significant drop in its amount up to 1180°C, of around 5wt%; then its content decreased with a slower rate. The batch with the minor content of ash, C2, really kept a constant rate of quartz dissolution along the ramp, while the trends of C4 and C6 are almost overlapping, apart from a first considerable reduction in C6 between 1100 and 1130°C, of around 4wt% of quartz. It can be inferred from these results that the increasing introduction of ash moderately affects the evolution of quartz. Actually, the relative variation of its contents in all the

batches – from the starting temperature up to the higher – is quite small, with a decrease of 7.3-7.5wt% for C0-C2 and 8.2-8.7wt% for C4-C6.

Feldspars – plagioclase plus K-feldspar – are the main ingredients of porcelain stoneware, playing the role of fluxing agents. In between 1000 and 1130°C, the contents of feldspars remained more stable the more ash is added, while in the C0 batch their content decreased fairly regularly in this range. Specifically, for batch C0 there is a significant drop in this temperature span, with a dissolution of ~15wt% of feldspars. Considering the waste-bearing batches, C2 with a decrease of 11wt%, shows an intermediate behavior between C0 and the other batches C4 and C6. In these latter samples, in fact, the amount of feldspars shows a very slow decrease for C4 (4wt%), while a stable content with no variation is observed for C6, sign of no dissolution in this temperature range. Starting from 1130°C onwards there is, for all the samples, a change in the slope of the curves with a significant increase in the melting kinetics, with a drop of ~30-35wt% of feldspars for all the bodies, in the range 1130-1220°C. Samples containing ash, as the temperature increased, retained more plagioclase than sample C0, with a direct correlation between the amount of ash introduced in the bodies and the residual plagioclase. Indeed, at the end of the ramp, at 1220°C, C0 shows a content of feldspar of ~2wt% *versus* those of the ash-bearing batches ranging from ~5 to 8wt%. This phenomenon sheds light on the behavior of the ash, beyond its fluxing role. BBA melted in place of the feldspars, allowing a greater amount to be preserved up to the maximum firing temperatures. Despite no data on quantitative mineralogical composition of ash-bearing batches are available in the literature, an analogous behavior has been observed for porcelain stoneware containing glassy wastes [56] and also strong fluxes [57]. Conte and co-workers [56] reported that porcelain stoneware bodies with 20wt% of different kinds of glassy waste (bottle, lamp, screen...) retained, after firing, more feldspars than the reference body. Similarly, also batches with strong fluxes – such as ulexite, colemanite, wollastonite and diopside in amount ≤10wt% – preserved a slightly higher amount of feldspars with respect to the standard [57].

Figure 9.

Mullite begins its crystallization at a temperature of about 1000°C, the growing rate of this phase is higher in the first range of temperature (1000-1100°C) for the waste-bearing bodies with respect to C0, which shows a delay of about 100°C. This delay is somehow compensated by a faster rate of crystallization in the range 1100-1200°C, which is higher than that showed by the waste-bearing bodies in the span 1000-1180°C. The maximum mullite content is reached for all the samples at the maximum densification temperature, i.e., 1180°C for C2-C4-C6 and 1200°C for the C0, even if in different amount (~7wt% for the ash-bearing bodies *versus* 9.5wt% for the benchmark). After

reaching the maximum densification temperature, the mullite appears to be unstable and its content slightly decreased in all the batches. At the best of our knowledge, no quantitative data on mullite contents are available for ceramic batches with ashes. Nevertheless, we can compare our data with those of porcelain stoneware obtained after the addition of glassy waste [56] and strong fluxes [57]. Results indicated that the introduction of raw materials rich in alkali and alkali-earths inhibits the mullite formation, decreasing its contents at the temperatures of maximum densification, if compared to the respective benchmarks.

Due to the breakdown of phyllosilicates, the incipient melting of feldspars and the partial melting of quartz, the amorphous phase increased with firing temperature, particularly from 1130°C onwards, when its amount passed from ~30-37wt%, to ~70wt% at 1220°C. The amount of glassy phase present in the bodies is different at the temperatures of maximum densification (1180°C, about 50-60% for samples with ash; 1200°C, 66% for C0), while it is almost the same for all samples at the maximum tested temperature (1220°C). Overall, the trend of the vitreous phase suggests a limited effect of BBA up to 4wt% and a more appreciable decreasing in content in C6.

Quantitative mineralogical data allowed to identify a temperature range characterized by massive phase transformations, whom gave rise to the sintering by viscous flow of the ceramic body. Indeed, between 1100 and 1130°C, the bulk density curves became steeper (Figure 7), indicating the acceleration of the densification process. Overall, the mineralogical data suggest that the introduction of BBA did not deeply influence the evolution of the phases. However, the observed variations of quartz, mullite and feldspars between the reference body and those with ash have some implications. The mechanism that guarantees the high temperature stability of the porcelain stoneware bodies requires the presence of a quartz and mullite skeleton inside a peraluminous melt. Any dissolution of the quartz skeleton would lead to a decrease in the viscosity of the mass, but is counterbalanced by the increasing viscosity of the liquid phase, due to the increase in its silica content [54]. If the skeleton is made up of feldspars, their dissolution, with release of alkali and alkali-earth, would lead to a drop in viscosity of the liquid phase and no counterbalancing effect would occur. This is the undesired phenomenon that limits the use of peralkaline raw materials (molar ratio $Al_2O_3/Na_2O+K_2O+CaO<1$).

3.4 Microstructure of fired porcelain stoneware tiles

To investigate the microstructure at various temperatures, corresponding to different sintering stages, scanning electron microscope analyses were carried out. Four different significant temperatures were selected: *i)* 1000°C for the start of the sintering process, corresponding to small tile size variation up to 1100°C; *ii)* 1130°C for the intermediate stage, characterized by formation of glassy ponds,

accounting for most densification up to the temperature of maximum density [58]; *iii)* the maximum densification of bodies at 1180°C for C2, C4, C6 and at 1200°C for C0; *iv)* 1220°C for overfiring.
At the lowest temperature considered (1000°C, Figure 10), all samples exhibit characteristics of un-sintered bodies. Specifically, a highly crystalline appearance is observed, characterized by several crystals with sharp edges, resulting from grinding, which represents the starting assemblage of feldspars and quartz grains dispersed into a fine-grained matrix that includes clay minerals and porosity.

Figure 10.

Figure 11 shows a detail of an image collected on the C6 sample, accompanied by EDS spectra collected on some points of interest. The high-contrast grain, analyzed in spectrum 1, is rich of iron, while the grain analyzed in point 2 is compatible with a K-feldspar, and grains at points 3-4 are quartz.

Figure 11.

At 1130°C (Figure 12) the C0 sample is still mainly characterized by crystals with a defined shape, while for the other bodies, the increase in temperature led to a significant loss of angularity and the formation of necks between the various grains, which suggest the occurrence of a liquid phase and the melting of feldspars and ash. As it can be seen from the graphs of phase evolution (Figure 9), it is indeed at this temperature that an abundant melting began, leading to the fast increase of the vitreous phase.

Figure 12.

At the temperature of maximum densification (Figure 13) all the batches show a compact microstructure with relics of quartz and feldspars crystals, rounded isolated pores (from a few μm up to ~20 μm in diameter) and irregularly shaped pores, presumably inherited from powder compaction defects. Crystals and pores are dispersed in an abundant vitreous phase (liquid at high temperature), which promoted the sintering process by wetting the mineral particles and reducing the voids, so increasing the bulk density of the ceramic tile. These microstructural features are typical of sintered porcelain stoneware [54,57]. In detail, it is possible to observe that the reference batch shows a lower volume of pores with respect to the other samples. Pores are, on average, also smaller in size.

Figure 13.

Similar features, with increasing in closed porosity – quantity and size – related to the growing content of ash, were observed also in batches containing diverse kinds of biomass ashes, but linked to different phenomenological processes. SEM micrographs of bodies containing sugarcane bagasse ash [16, 22]

revealed an increasing in closed pores explained by the combustion of the organic fraction of the ashes. TG curve indicates that ash-bearing batch had significant mass loss (LOI ~12wt%), mostly matching the exothermic event around 580°C related to the decomposition and oxidation of organic compounds (charcoal and organic matter), with the release of CO_2 [22]. Otherwise, the increasing in porosity recorded for batches containing coffee husk ash, could be related to the decomposition of calcium carbonate, which occurs with significant weight loss (~20wt%) associated with a strong endothermic event, between 825 and 1090°C [30]. The behaviour of bodies which incorporate rice straw ash [14,29], is much more similar to that of the batches studied here. In fact, they are characterized by a significantly lower LOI with respect to both sugarcane bagasse ash and coffee husk ash (Table 1). In this case, the gas development might be due to the high content of gas-generating substances such as Cl for rice straw ash and calcite and Fe_2O_3 for BBA, which, in combination with the narrow vitrification range, led to swelling of the body.

The intensification of this phenomenon can be observed in our samples passing to 1220°C (Figure 14). At this temperature it appears clear how the technological properties are affected by the microstructure, which took the traits of the over-firing. Indeed, the inversion of shrinkage trend and the significant loss of bulk density for the waste-bearing batches (Figures 6-7) are mirrored in SEM micrographs by a pore coarsening effect. Large pores, with a diameter up to 60 μm, clearly testify the occurrence of de-sintering processes related to bloating phenomena, which can foster pyroplastic deformations. On the other hand, the benchmark C0 exhibits a good stability at the highest temperature with respect to the other batches, as also testified by the HSM stability test (Figure 8), even if an incipient pore coarsening can be appreciated.

Figure 14.

4. CONCLUSIONS

This study investigated the feasibility of biomass bottom ash recycling in porcelain stoneware bodies, offering ~~for the first time~~ a comprehensive analytical approach from the technological, mineralogical and microstructural point of views. ~~The simulation of the industrial cycle at the laboratory scale allowed to evaluate the effect of the ash introduction at any step of the ceramic tiles production, while the quantitative mineralogical and SEM data of the tiles fired at different temperatures, allowed to understand the way by which the biomass ash affects the viscous sintering.~~

Due to its physical-chemical properties, the BBA was introduced in the ceramic batch in partial substitution of feldspars, up to 6wt%. The simulation of all the industrial tile manufacturing process allowed to highlight for the first time a bottleneck related to the rheological behavior of the slips. The presence of ashes, in fact, induced a considerable increase in the viscosity of the slip during the wet

milling, which was overcome by a slight addition of deflocculant, for a total of 0.6wt% on the dry mass. This hindrance was not pointed out in previous studies, since the ashes are usually added by dry route to the ceramic batches. This work demonstrated that this obstacle present in the wet milling process, typically used in the industrial practice, can be easily managed.

There were no further technological drawbacks in the process simulation. Moreover, no significant variations with respect to technological parameters, such as particle size distribution, springback, green and dry bulk density were identified, indicating that the introduction of ash, within certain limits, guarantees the maintenance of the required properties of the semi-finished products along the production line. As far it concerns the firing behavior, the introduction of ash allowed to lower the firing temperature by 20°C (1180°C) with respect to the waste-free batch (1200°C), while maintaining good levels of densification, with bulk density around 2.4 g/cm^3. However, it was noticed a tendency of the waste-bearing batches to instability at high temperatures, so that the gresification window tends to be rather narrow. As known, in fact, the power in reducing the temperature of maximum densification assigns to the biomass ashes the role of fluxing agents, but their increasing amount in the ceramic batches can cause a fast decrease in bulk density ~~[14,16-17,22,29-30]~~. In this sense, it is important to identify the exact firing temperature of the bodies, in order not to incur phenomena related to the over-firing of ceramic products, such as bloating, as suggested by SEM and HSM results.

The study of the phase evolution at different firing temperatures, permitted to unveil different behaviors. The introduction of ash led to a delay in feldspars melting of about 100°C compared to the reference sample; at the same time, already at 1000°C, the glassy phase appears to be higher in the samples with ash, probably because BBA induced melting reactions at lower temperature with respect to the feldspars. Moreover, the presence of bottom ash led to persistence of more feldspars at the end of firing with respect to ~~sample C0~~ the waste-free body. This is thought to occur since ash melt in place of the feldspars, leaving a larger amount of these minerals at the end of the process. Even if, as far as we know, no quantitive data of the mineralogical composition of ashes-bearing bodies are available, a similar behaviour, with the waste melting in place of feldspars, was already osebrved for glassy wastes ~~[56]~~ and alternative strong fluxes ~~[57]~~.

The addition of ash to the batches, in partial replacement of the classical fluxes, speeded up the sintering process, leading to the early formation of the amorphous phase and the decreasing of the maximum temperature of densification ~~(20°C lower than the benchmark)~~. Effects of this "anticipation" can also be read in the SEM images. The micrographs revealed how phase evolution coincides with the microstructure evolution, so samples show different textural characteristics at the same temperature, coinciding with different sintering stage.

Taking into account all the collected data, the ceramic product obtained from ~~C4~~ the batch containing 4wt% of bottom ash is the best choice among the tested ones, showing values perfectly matching the standard requirements for porcelain stoneware. In contrast, the 6wt% replacement represents the limit of introduction for this type of formulation. The results obtained are therefore promising from an industrial point of view, and demonstrate for the first time the feasibility of biomass bottom ash recycling in porcelain stoneware bodies along all the production line, with small variation just in the step of the wet milling. ~~Anyway, it should be remembered that the chemical and mineralogical composition of biomass bottom ashes is extremely variable, depending not only on the biomass of origin but also on the processes with which were generated. The characterizations of the ashes themselves before their employ are therefore of fundamental importance. On the other hand, it should be also remembered that these ashes are classified by the CER code (European waste catalog, directive 75/442/EEC) as non-hazardous materials, and, in force of this and the maintenance of the required properties for semi-finished and finished ceramic products (with the potential lowering of the firing temperatures), they represent an excellent candidate for further technological investigations.~~

ACKNOWLEDGEMENTS

This work was undertaken within the CNR project "*Capitale naturale e risorse per il futuro dell'Italia (FOE 2020)*" as deliverable "*Utilizzo razionale di risorse tramite riduzione di materia prime critiche, valorizzazione degli scarti e riciclo efficace*" (Dipartimento di Scienze Chimiche e Tecnologie dei Materiali – DSCTM). *CUP=B85F21002120005*

REFERENCES

[1] Baraldi, L. (2019). World production and consumption of ceramic tiles. Ceramic World Review, 133, 48–63.

[2] Dondi, M., García-Ten, J., Rambaldi, E., Zanelli, C., Vicent-Cabedo, M. (2021). Resource efficiency versus market trends in the ceramic tile industry: Effect on the supply chain in Italy and Spain. Resources, Conservation and Recycling, 168, 105271.

[3] Palmonari, C., Timellini, G. (2000). Environmental impact of the ceramic tile industry. New approaches to the management in Europe. Ceramica Acta 12 (4), 16–35.

[4] Blengini, G.A., Shields, D.J. (2010). Green labels and sustainability reporting: Overview of the building products supply chain in Italy. Management of Environmental Quality: An International Journal 21 (4), 477–493.

[5] Gabaldón-Estevan, D., Criado, E., Monfort, E. (2014). The green factor in European manufacturing: a case study of the Spanish ceramic tile industry. Journal of Cleaner Production 70, 242–250.

[6] WGBC (2022). World Green Building Council. https://www.worldgbc.org/ [last accessed on January 26, 2022].
[7] ISO 17889 (2021). Ceramic tiling systems — Sustainability for ceramic tiles and installation materials — Part 1: Specification for ceramic tiles. International Organization for Standardization.
[8] Andreola, N.M.F., Barbieri, L., Lancellotti, I., Leonelli, C., Manfredini, T. (2016). Recycling of industrial wastes in ceramic manufacturing: State of art and glass case studies. Ceramics International 42 (12), 13333–13338.
[9] Coronado, M., Blanco, T., Quijorna, N., Alonso-Santurde, R., Andrés, A. (2015). Types of waste, properties and durability of toxic waste-based fired masonry bricks. Eco- Efficient Masonry Bricks and Blocks. Woodhead Publishing, 129–188.
[10] Coronado, M., Segadães, A.M., Andrés, A. (2015). Using mixture design of experiments to assess the environmental impact of clay-based structural ceramics containing foundry wastes. Journal of Hazardous Materials 299, 529–539.
[11] Cifrian, E., Coronado, M., Quijorna, N., Alonso-Santurde, R., Andrés, A. (2019). Waelz slag-based construction ceramics: effect of the trial scale on technological and environmental properties. Journal of Material Cycles and Waste Management, 21 (6), 1437–1448.
[12] Zanelli, C., Conte, S., Molinari, C., Soldati, R., Dondi, M. (2021). Waste recycling in ceramic tiles: a technological outlook. Resources, Conservation & Recycling 168, 105289.
[13] Guzman, A., Torres, J., Cedeno, M., Delvasto, S., Borras, V.A., Vilches E.J.S. (2013). Fabricacion de gres porcelanico empleando ceniza de tamo de arroz en sustitucion del feldespato. Boletín de la Sociedad Espãnola de Ceramica y Vidrio 52 (6), 283–290.
[14] Guzman, A., Delvasto, A., Francisca Quereda, V. M., Sanchez, V. (2015). Valorization of rice straw waste: production of porcelain tiles. Ceramica 61 (360), 442–449.
[15] Amutha, K., Sivakumar, G., Elumalai, R. (2014). Comparison studies of quartz and biosilica influence on the porcelain tiles. International Journal of Scientific and Engineering Research 5 (3), 102–105.
[16] Schettino, M.A., Holanda, J.N. (2015). Processing of porcelain stoneware tile using sugarcane bagasse ash waste. Processing and Application of Ceramics 9 (1), 17–22.
[17] Abeid, S., Park, S.E. (2018). Suitability of vermiculite and rice husk ash as raw materials for production of ceramic tiles. International Journal of Materials Science and Applications 7 (2), 39.
[18] Olokode, O.S., Aiyedun, P.O., Kuye, S.I., Anyanwu, B.U., Eng, B., Owoeye, F.T., Adekoya, T.A. (2013). Optimization of the quantity of wood ash addition on kaolinitic clay performance in porcelain stoneware tiles. Pacific Journal of Science and Technology 14 (1), 48–56.

[19] Paranhos, R.J.S., Acchar, W., Silva, V.M. (2017). Use of sugarcane bagasse ashes as raw material in the replacement of fluxes for applications on porcelain tile. Materials Science Forum 881, 383–386.
[20] Fernandes, H.R., Ferreira, J.M.F. (2007). Recycling of chromium-rich leather ashes in porcelain tiles production. Journal of the European Ceramic Society 27 (16), 4657–4663.
[21] Andreola, N.M.F., Martín, M.I., Ferrari, A.M., Lancellotti, I., Bondioli, F., Rincon, J.M., Romero, M., Barbieri, L. (2013). Technological properties of glass-ceramic tiles obtained using rice husk ash as silica precursor. Ceramics International 39 (5), 5427–5435.
[22] Faria, K.C.P., Holanda, J.N.F. (2016). Thermal behavior of ceramic wall tile pastes bearing solid wastes. Journal of Thermal Analysis and Calorimetry 123 (2), 1119–1127.
[23] Jamo, H.U., Noh, M.Z., Ahmad, Z.A. (2015). Effects of mould pressure and substitution of quartz by palm oil fuel ash on compressive strength of porcelain. Advanced Materials Research 1087, 121–125.
[24] Barbieri, L., Corradi, A, Lancellotti, I., Manfredini, T. (2002). Use of municipal incinerator bottom ash as sintering promoter in industrial ceramics. Waste Management, 22, 859–863.
[25] Bourtsalas, A., Vandeperre, L.J., Grimes, S.M., Themelis, N., Cheeseman, C.R. (2015). Production of pyroxene ceramics from the fine fraction of incinerator bottom ash. Waste Management, 45, 217- 225.
[26] Dana, K., Dey, J., Das, S.K. (2005). Synergistic effect of fly ash and blast furnace slag on the mechanical strength of traditional porcelain tiles. Ceramics international 31 (1), 147–152.
[27] Wang, H., Zhu, M., Sun, Y., Ji, R., Liu, L., Wang, X. (2017). Synthesis of a ceramic tile base based on high-alumina fly ash. Construction and Building Materials 155, 930–938.
[28] Dana, K., Das, S.K. (2002). Some studies on ceramic body compositions for wall and floor tiles. Transactions of the Indian Ceramic Society 61 (2), 83–86.
[29] Guzmán, Á., Gordillo, S.M., Delvasto, A.S., Quereda, V.M.F., Sánchez, V.E. (2016). Optimization of the technological properties of porcelain tile bodies containing rice straw ash using the design of experiments methodology. Ceramics International, 42(14), 15383- 15396.
[30] Acchar, W., Dultra, E.J.V., Segadães, A.M. (2013). Untreated coffee husk ashes used as flux in ceramic tiles. Applied Clay Science 75-76, 141–147.
[31] Acchar, W., Avelino, K.A., Segadães, A.M. (2016). Granite waste and coffee husk ash synergistic effect on clay-based ceramics. Advances in Applied Ceramics 115 (4), 236–242.
[32] Acchar, W., Dultra, E.J. (2015). Porcelain tile. Ceramic Materials from Coffee Bagasse Ash Waste. Springer International Publishing, 3–15.

[33] Carvalho, V.H.M., Rocha, M.B.S., Dultra, E.J.V., Acchar, W., Segadães, A.M. (2017). Beneficiation of coffee husk ashes to be used as flux in porcelain tiles. Proceedings 4th WASTES: Solutions, Treatments and Opportunities, September 25-26, 2017, Guimarães, Portugal, 2-4.
[34] Sivakumar, G., Hariharan, V., Shanmugam, M., Mohanraj, K. (2014). Fabrication and properties of bagasse ash blended ceramic tiles. International Journal of ChemTech Research, 6(12), 4991-4994.
[35] Noh, M.Z., Jamo, H.U., Ahmad, Z.A. (2014). Effect of temperature and composition of palm oil fuel ash on compressive strength of porcelain. Applied Mechanics and Materials, 660, 173-177.
[36] Aripin, A., Tani, S., Mitsudo, S., Saito, T., Idehara, T. (2010). Fabrication of unglazed ceramic tile using dense structured sago waste and clay composite. Indonesian Journal of Materials Science 11 (2), 79–82.
[37] Novais, R.M., Seabra, M.P., Labrincha, J.A. (2015). Wood waste incorporation for lightweight porcelain stoneware tiles with tailored thermal conductivity. Journal of Cleaner Production 90, 66–72.
[38] Naga, S.M., Awaad, M., El-Mehalawy, N., Antonious, M.S. (2014). Recycling of fish bone ash in the preparation of stoneware tiles. International Ceramic Review 63 (1-2), 15–18.
[39] Awaad, M., Naga, S.M., El-Mehalawy, N. (2015). Effect of replacing weathered feldspar for potash feldspar in the production of stoneware tiles containing fish bone ash. Ceramics International 41 (6), 7816–7822.
[40] European waste catalog, directive 75/442/EEC. ICER INTERNATIONAL. Research and Innovation Portal and of the circular economy https://www.icer-grp.com/index.php/en/services/tecnopedia-en/information-on-ewc-codes [last accessed on January 26, 2022].
[41] Gualtieri, A. F., Mazzucato, E., Venturelli, P., Viani, A., Zannini, P., Petras, L. (1999). X-ray Powder Diffraction Quantitative Analysis Performed in Situ at High Temperature: Application to the Determination of NiO in Ceramic Pigments. Journal of Applied Crystallography, 32, 808-813.
[42] Larson, A.C., Von Dreele, R.B. (1994). General structure analysis system "GSAS". Los Alamos National Laboratory Report, Los Alamos, LAUR 86−748.
[43] Toby, B.H. (2001). EXPGUI, A graphical user interface for GSAS. Journal of Applied Crystallography, 34, 210−213.
[44] Modolo, R.C.E., Tarelho, L.A.C., Teixeira, E.R., Ferreira, V.M., Labrincha, J.A. (2014). Treatment and use of bottom bed waste in biomass fluidized bed combustors. Fuel Processing Technology 125, 170-181.

[45] Cabrera, M., Galvin, A.P., Agrela, F., Carvajal, M.D., Ayuso, J. (2014). Characterisation and technical feasibility of using biomass bottom ash for civil infrastructures. Construction and Building Materials, 58, 234-244.
[46] Khan, A., Jong, W., Jansens, P., Spliethoff, H. (2009). Biomass combustion in fluidized bed boilers: Potential problems and remedies. Fuel Processing Technology 90, 21–50.
[47] Hinojosa, M.J.R., Galvın, A.P., Agrela, F., Perianes, M., Barbudo, A. (2014). Potential use of biomass bottom ash as alternative construction material: conflictive chemical parameters according to technical regulations. Fuel 128, 248-259.
[48] Sklivaniti, V., Tsakiridis, P.E., Katsiotis, N.S., Velissariou, D., Pistofidis, N., Papageorgiou, D. (2017). Valorisation of woody biomass bottom ash in Portland cement: a characterization and hydration study. Journal of Environmental Chemical Engineering. 5 (1), 205-213.
[49] Vassilev, S.V., Baxter, D., Andersen, L.K., Vassileva, C.G. (2013). An overview of the composition and application of biomass ash. Part 1. Phase-mineral and chemical composition and classification. Fuel 105, 40-76.
[50] Nurmesniemi, H., Manskinen, K., Pöykiö, R, Dahl, O. (2012). Fertilizer properties of the bottom ash and fly ash from a large-sized (115 mw) industrial power plant incinerating wood-based biomass residues. Journal of the University of Chemical Technology and Metallurgy, 47, 1, 43-52.
[51] Dondi, M., Guarini, G., Conte, S., Molinari, C., Soldati, R., Zanelli, C. (2019). Deposits, composition and technological behavior of fluxes for ceramic tiles. Periodico di Mineralogia, 88, 235-257.
[52] Zanelli, C., Domínguez, E., Iglesias, C., Conte, S., Molinari, C., Soldati, R., Guarini, G., Dondi, M. (2019). Recycling of residual boron muds into ceramic tiles. Boletín de la Sociedad Española de Cerâmica y Vidrio 58 (5), 199–210.
[53] Sánchez, E., Garcia-Ten, J., Sanz, V., Moreno, A. (2010). Porcelain tile: Almost 30 years of steady scientific-technological evolution. Ceramics International, 36, 831–45.
[54] Conte, S., Zanelli, C., Ardit, M., Cruciani, G., Dondi, M. (2020). Phase evolution during reactive sintering by viscous flow: Disclosing the inner workings in porcelain stoneware firing. Journal of the European Ceramic Society, 40, 1738–1752.
[55] Devineau, K., Pichavant, M., Villiéras, F. (2005). Melting kinetics of granitic powder aggregates at 1175 C°, 1 atm. European Journal of Mineralogy, 17, 387–398.
[56] Conte, S., Zanelli, C., Molinari, C., Guarini, G., Dondi, M. (2020). Glassy wastes as feldspar substitutes in porcelain stoneware tiles: Thermal behaviour and effect on sintering process. Materials Chemistry and Physics, 256, 123613.

[57] Tavares Brasileiro, C., Conte, S., Contartesi, F., Gomes Melchiades, F., Zanelli, C., Dondi, M., Ortega Boschi, A. (2021). Effect of strong mineral fluxes on sintering of porcelain stoneware tiles. Journal of the European Ceramic Society, 41, 5755–5767.
[58] Zanelli, C., Raimondo, M., Dondi, M., Guarini, G., Tenorio, P. (2004). Sintering mechanisms of porcelain stoneware tiles. Proceedings Qualicer 2004, 247-259.

TABLES

Table 1. Chemical composition of ashes from combustion of biomasses of different sources.

% wt.	Sugarcane bagasse ash [16,19,22,34]	Sago ash [36]	Palm oil ash [35]	Coffee husk ash [33]	Rice husk ash [28]	Rice straw ash [14,29]	Fish bone ash [38]	Wood ash [18]	Biomass bottom ash [This work]
SiO_2	62.25	68.03	66.91	13.86	90.23	73.68	0.77	42.85	43.10
TiO_2	0.80	0.03	-	0.26	0.13	-	0.04	-	0.45
Al_2O_3	6.88	6.93	6.44	4.47	1.07	0.22	0.61	-	8.71
Cr_2O_3	-	0.04	-	-	-	-	-	-	0.02
Fe_2O_3	5.34	0.76	5.72	1.63	0.27	0.31	0.06	6.13	4.45
MgO	2.50	2.39	3.13	13.22	0.18	1.68	0.88	0.65	4.40
CaO	6.76	14.88	5.56	35.19	0.39	2.22	59.26	27.93	27.58
MnO	0.12	0.65	-	0.15	-	0.60	-	2.40	0.14
CuO	-	-	-	-	-	0.01	-	-	0.03
ZnO	-	-	-	-	-	0.04	0.02	0.44	0.01
SrO	-	-	-	0.25	-	0.01	0.17	-	0.11
BaO	-	-	-	-	-	0.06	-	-	0.04
Na_2O	0.41	1.35	0.19		-	0.39	0.74	0.67	1.20
K_2O	7.68	1.35	5.20	11.76	1.36	13.12	0.11	4.54	5.36
P_2O_5	1.41	1.66	3.72	9.85	3.83	2.56	36.84	-	1.44
SO_3	1.08	2.02	0.33	0.28	-	1.42	0.30	-	0.04
Cl	-	-	-	0.12	-	0.99	0.08	-	0.01
L.o.I.	7.72	-	2.30	9.82	3.83	1.84	-	13.73	3.17

Table 2. Formulations of the batches and their chemical composition (wt%) calculated considering the contribution by weight of each raw material.

%wt		**C0**	**C2**	**C4**	**C6**
PLASTIC COMPONENT	Ball clay A	20	20	20	20
	Ball clay B	20	20	20	20
FLUXES	Sodic feldspar	35	34	33	32
	Potassic feldspar	10	9	8	7
FILLER	Quartz-feldspathic sand	7	7	7	7
	Silica sand	8	8	8	8
BIOMASS BOTTOM ASH	BBA	0	2	4	6
SiO_2		69.77	69.23	68.69	68.15
Al_2O_3		18.87	18.69	18.51	18.33
TiO_2		0.60	0.61	0.61	0.62
Fe_2O_3		0.54	0.62	0.71	0.79
CaO		0.44	0.97	1.51	2.05
MgO		0.35	0.43	0.51	0.59
K_2O		2.25	2.29	2.32	2.36
Na_2O		4.03	3.93	3.84	3.74
P_2O_5		<0.01	0.03	0.06	0.09
MnO		<0.01	<0.01	0.01	0.01
Loss on Ignition (LOI)		3.16	3.20	3.25	3.30

Table 3. Technological properties of unfired products.

Property	unit	C0			C2			C4			C6		
Particle size d_{50}	µm	3.3	±	0.0	3.8	±	0.0	3.8	±	0.0	3.9	±	0.0
Springback	cm/m	0.50	±	0.02	0.47	±	0.02	0.45	±	0.01	0.44	±	0.02
Green bulk density	g/cm^3	2.066	±	0.003	2.130	±	0.013	2.149	±	0.012	2.145	±	0.005
Dry bulk density	g/cm^3	1.936	±	0.004	1.993	±	0.003	2.008	±	0.012	1.993	±	0.004

Figure 1

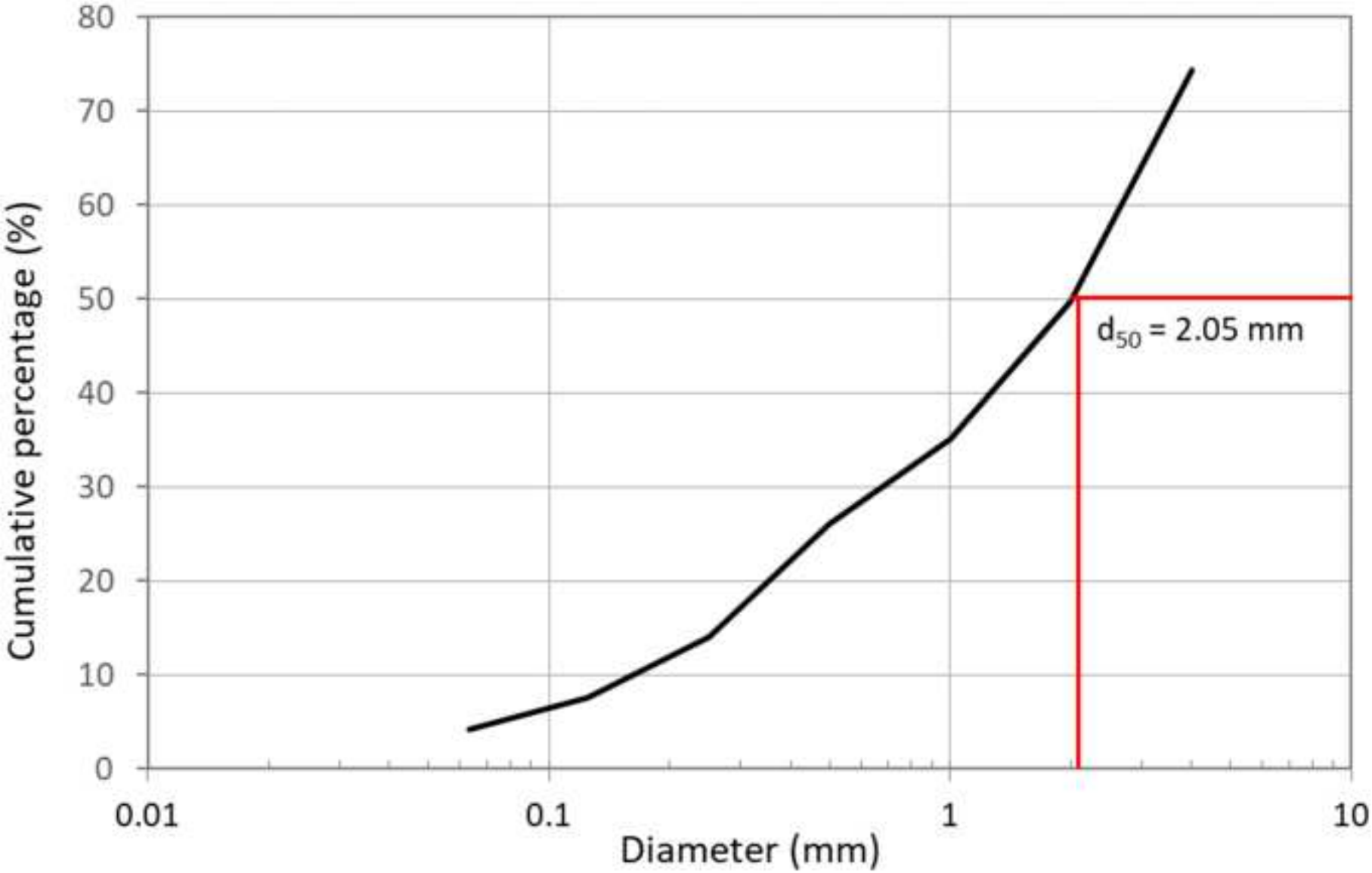

Figure 2

Click here to access/download;Figure;fig2.tiff

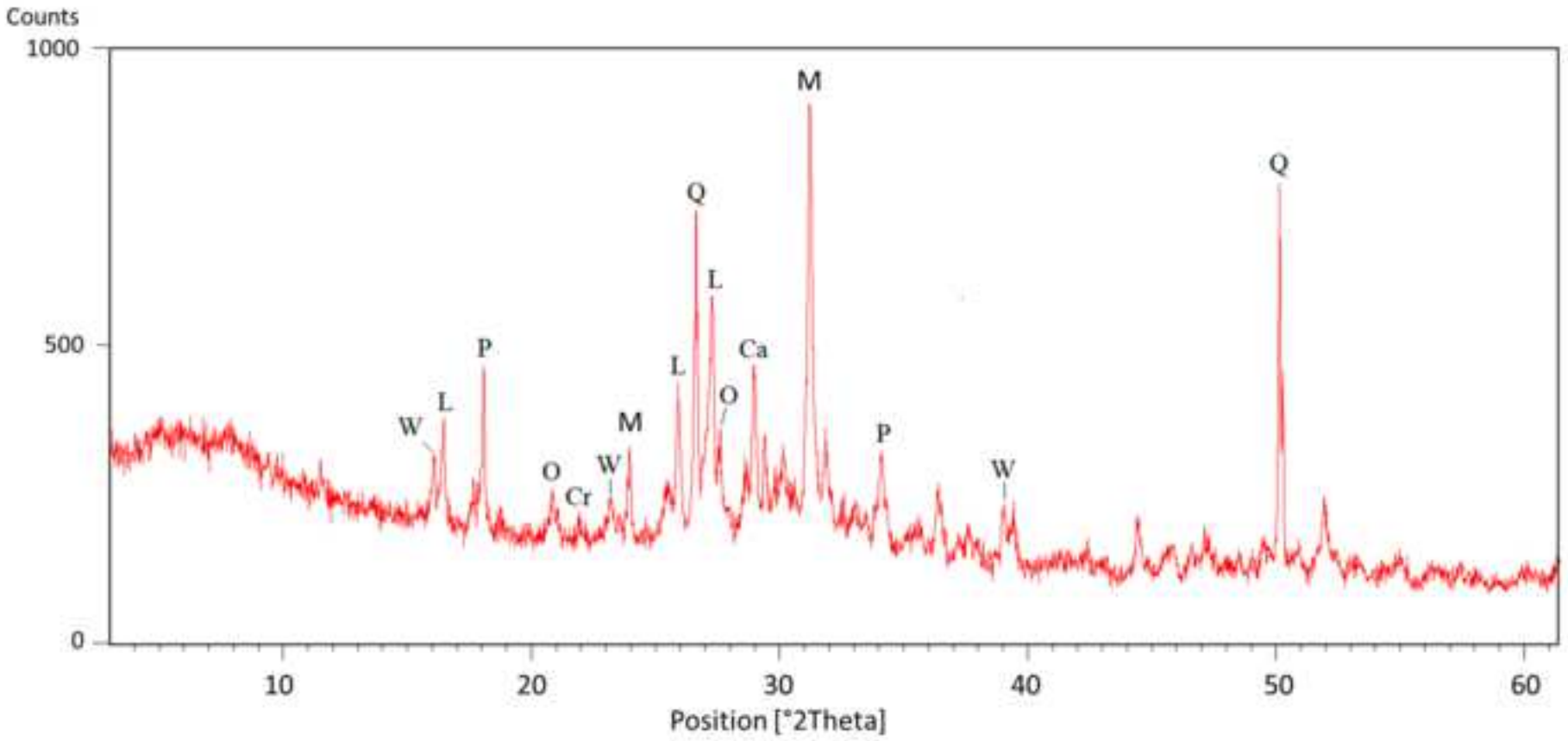

Figure 3

Click here to access/download;Figure;fig3.tiff

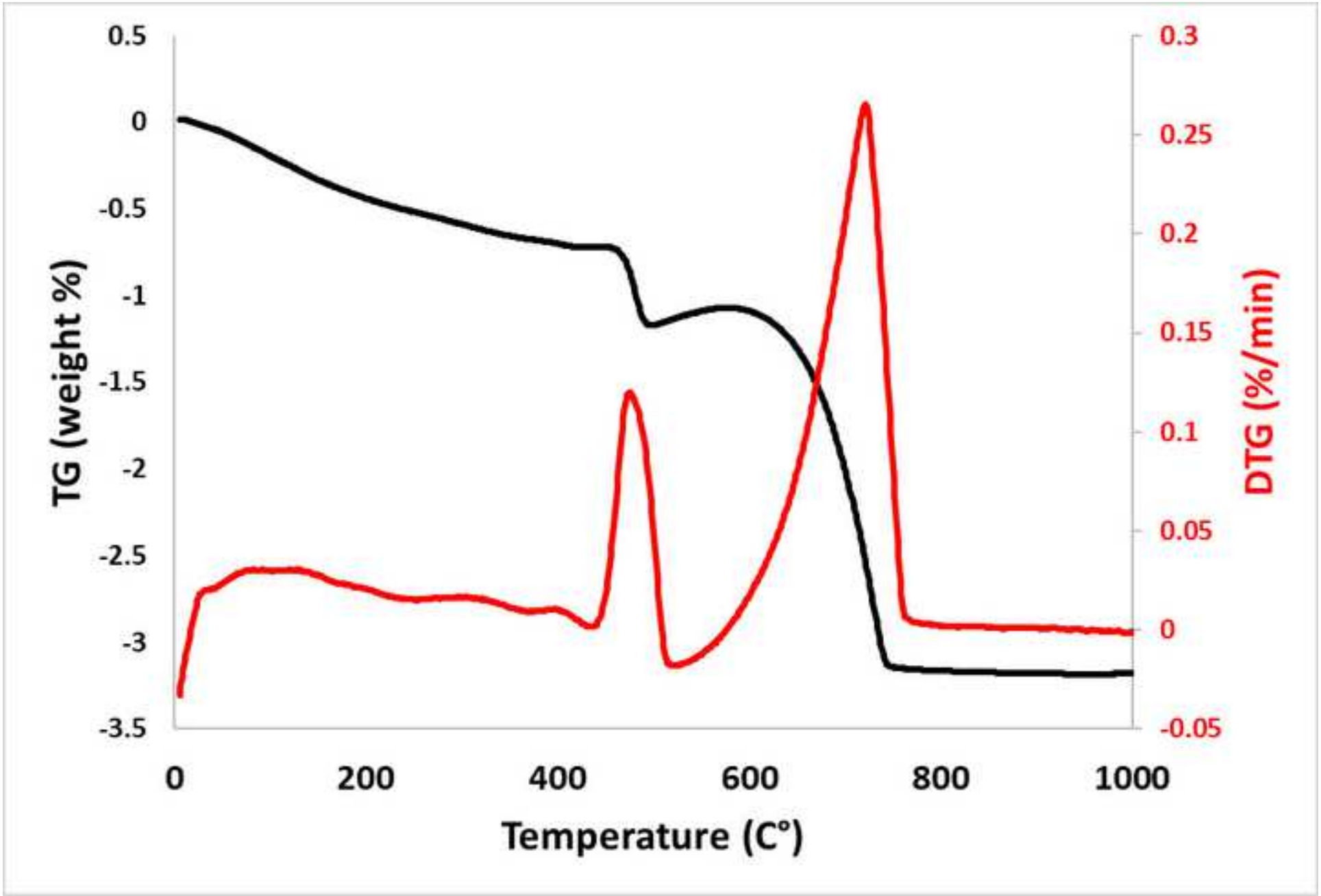

Figure 4

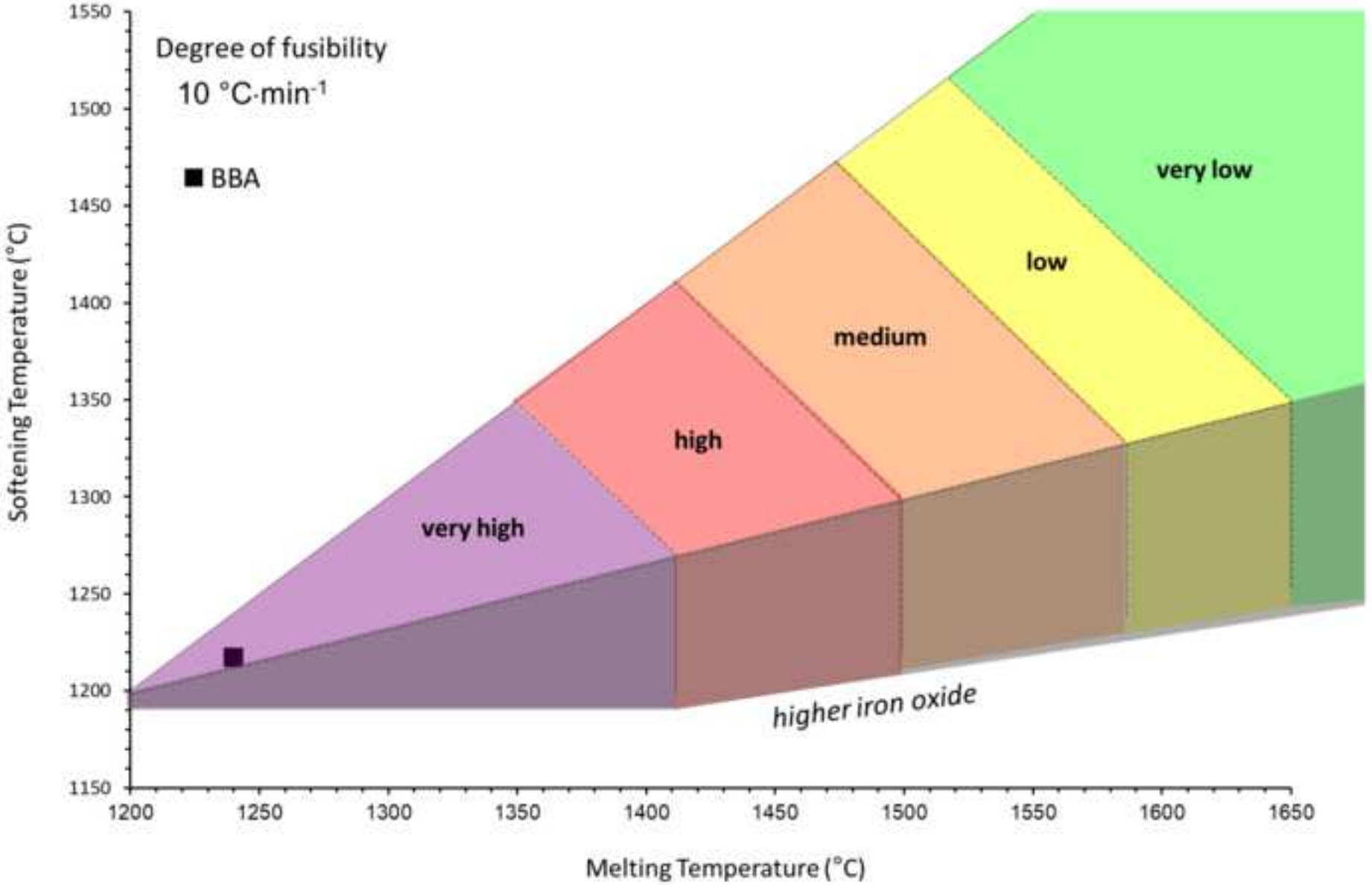

Figure 5

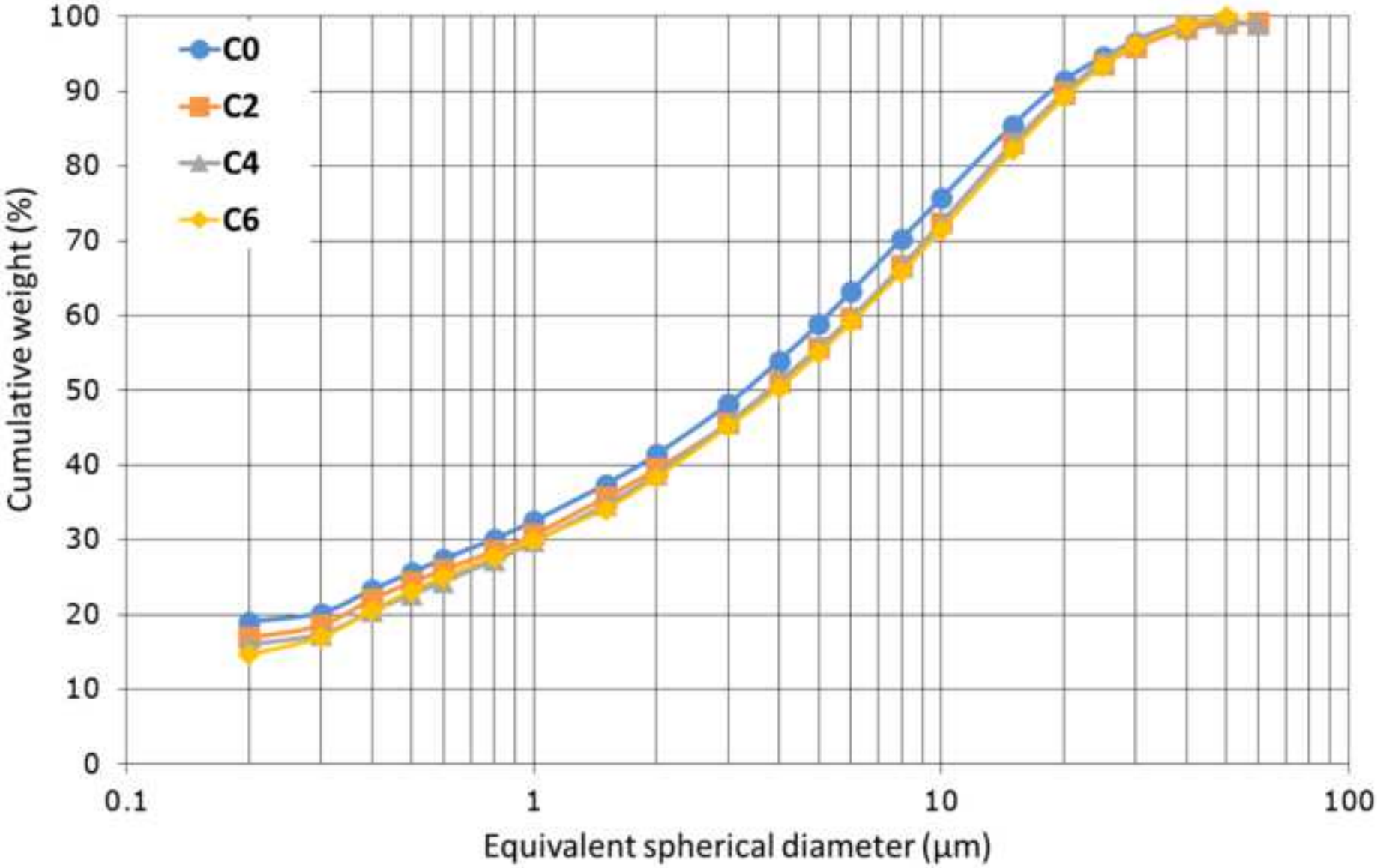

Figure 6

Click here to access/download;Figure;fig6.tiff

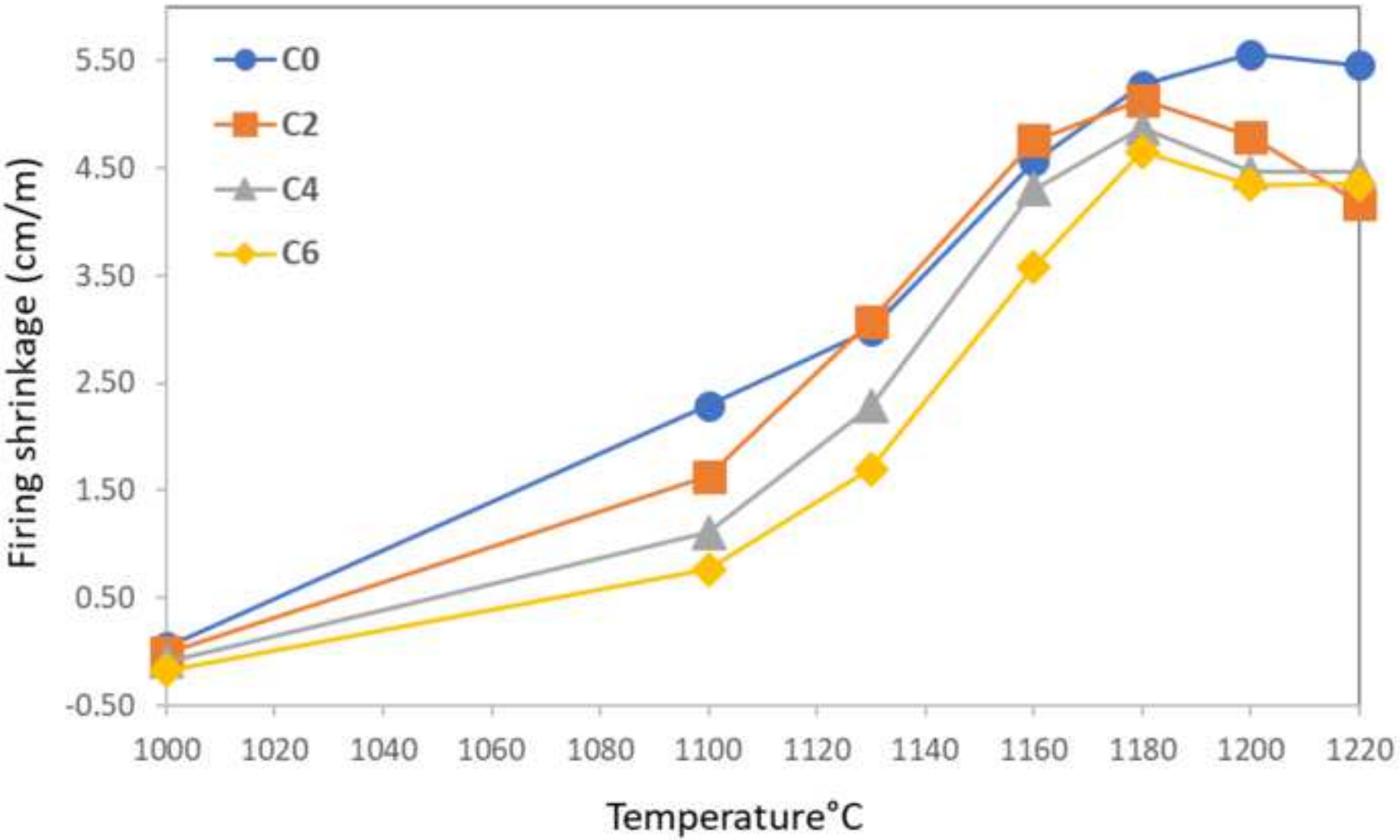

Figure 7

Click here to access/download;Figure;fig7.tiff

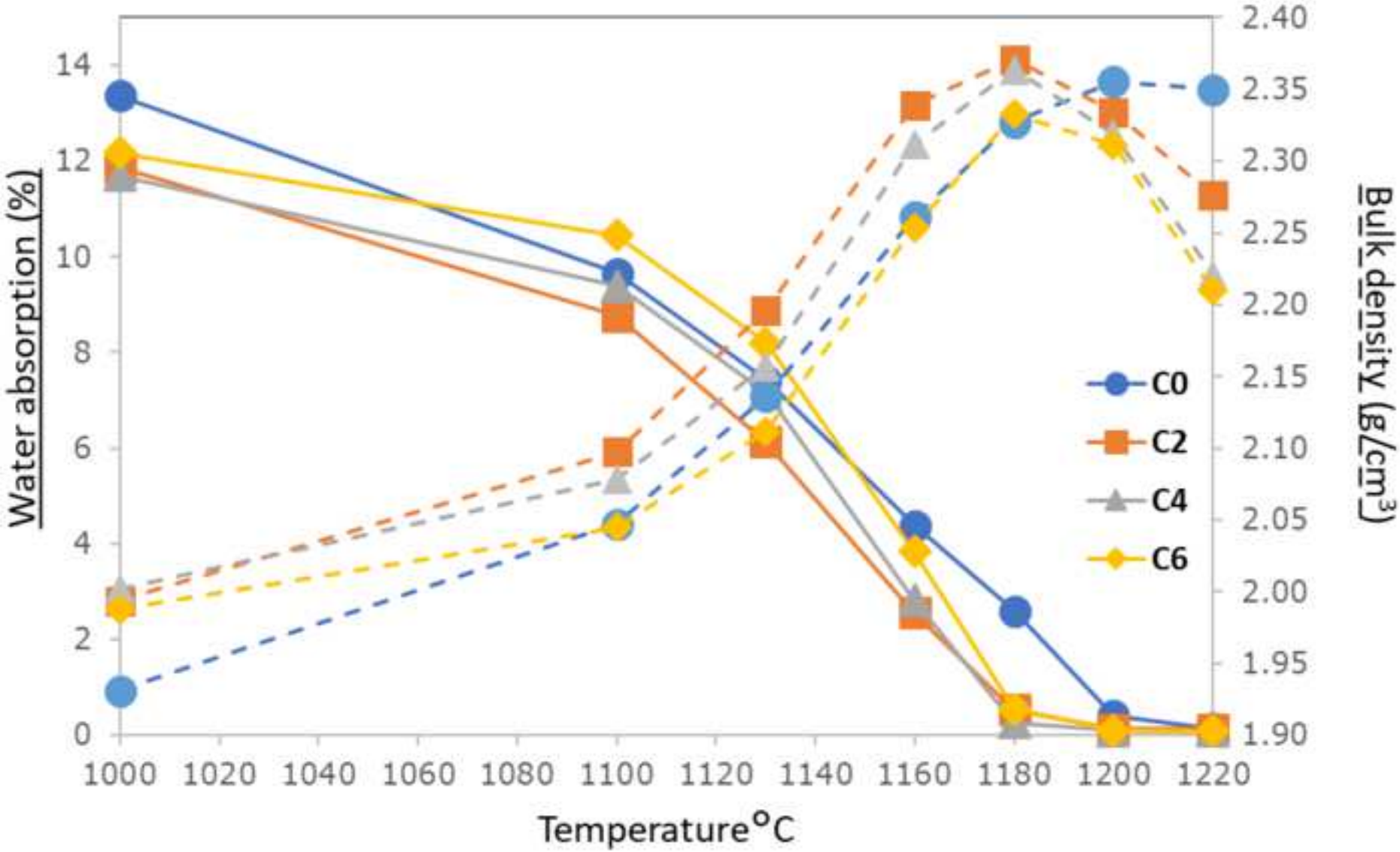

Figure 8

Click here to access/download;Figure;fig8.tiff

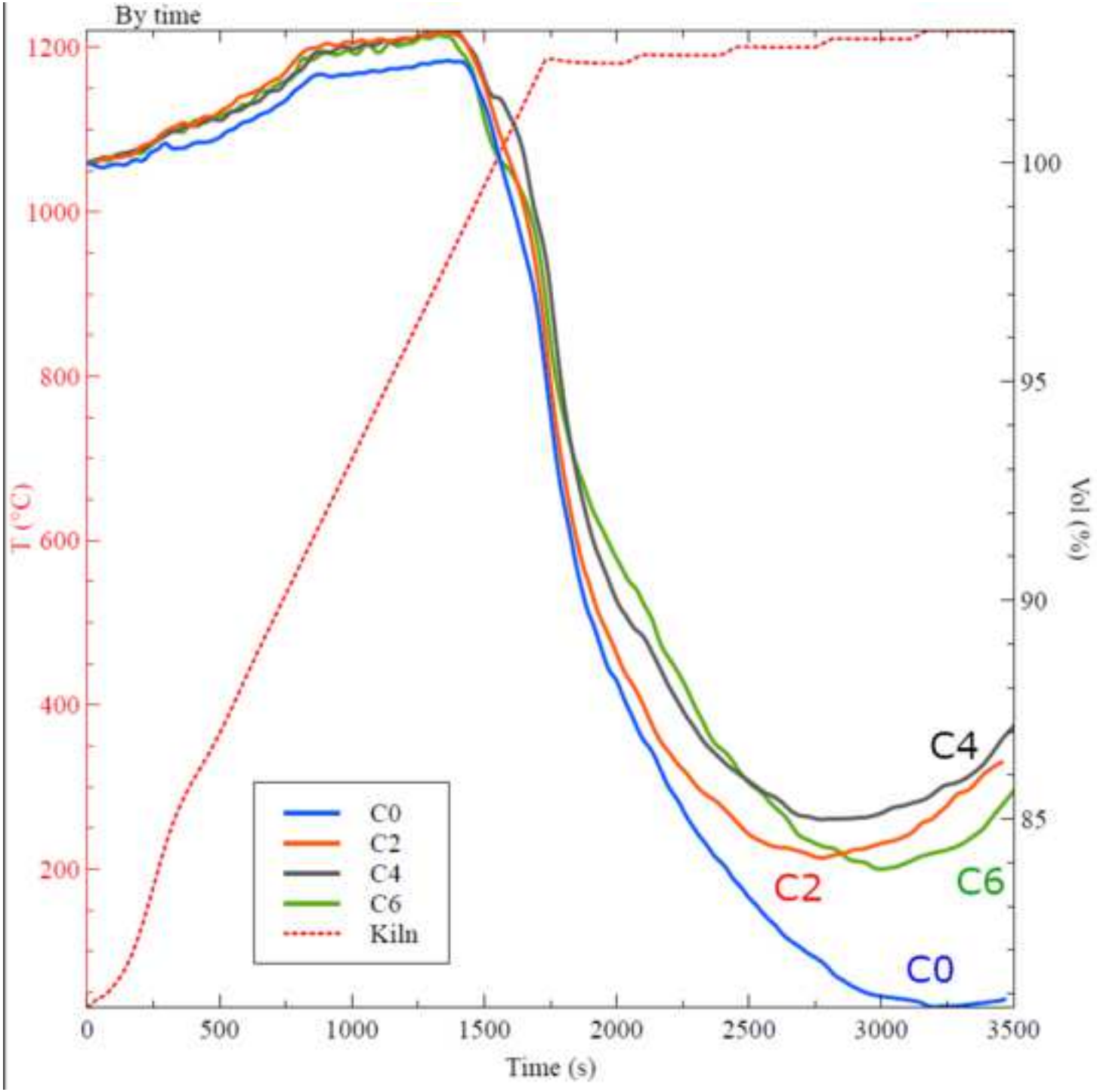

Figure 9

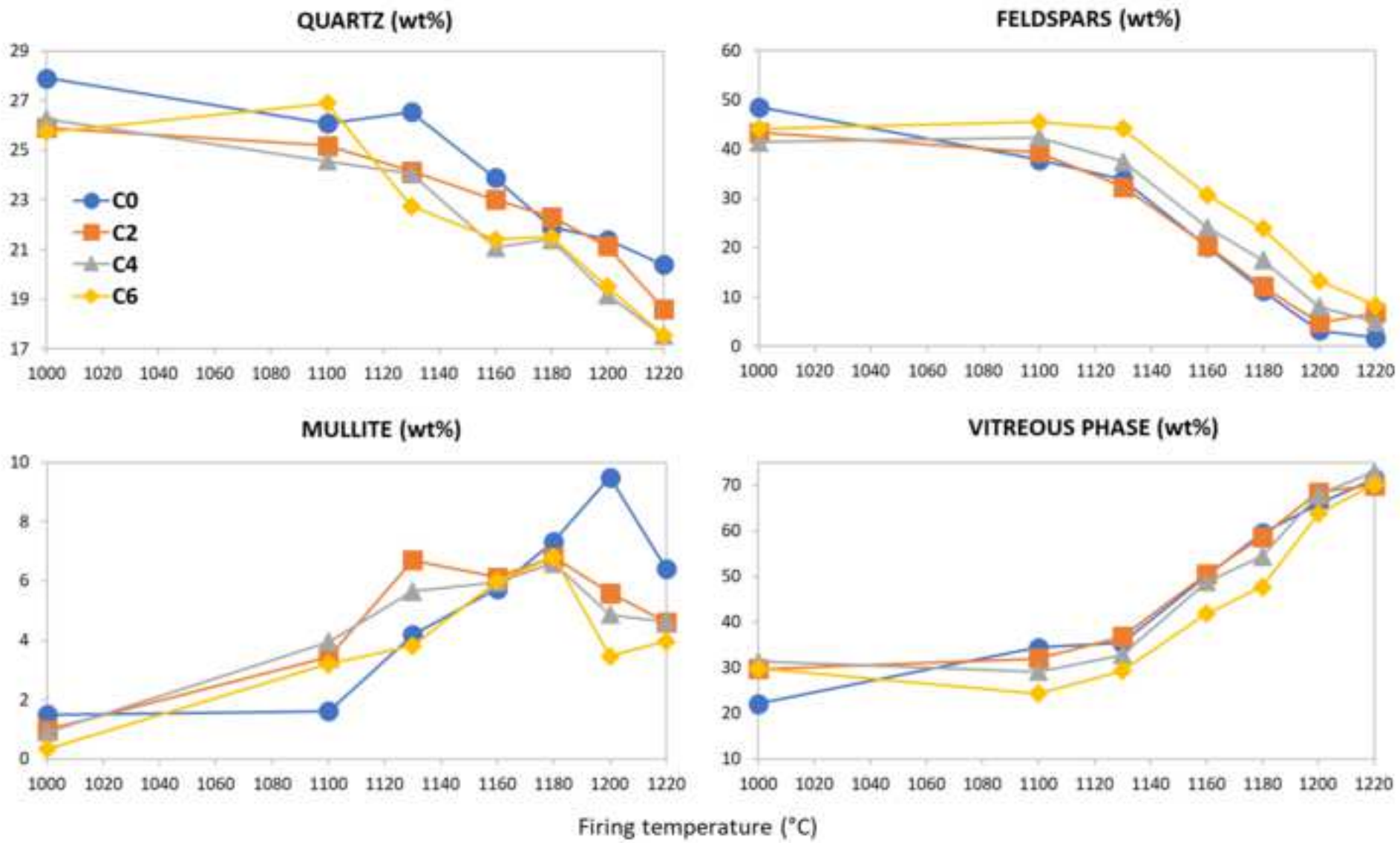

Figure 10

Click here to access/download;Figure;fig10.tiff

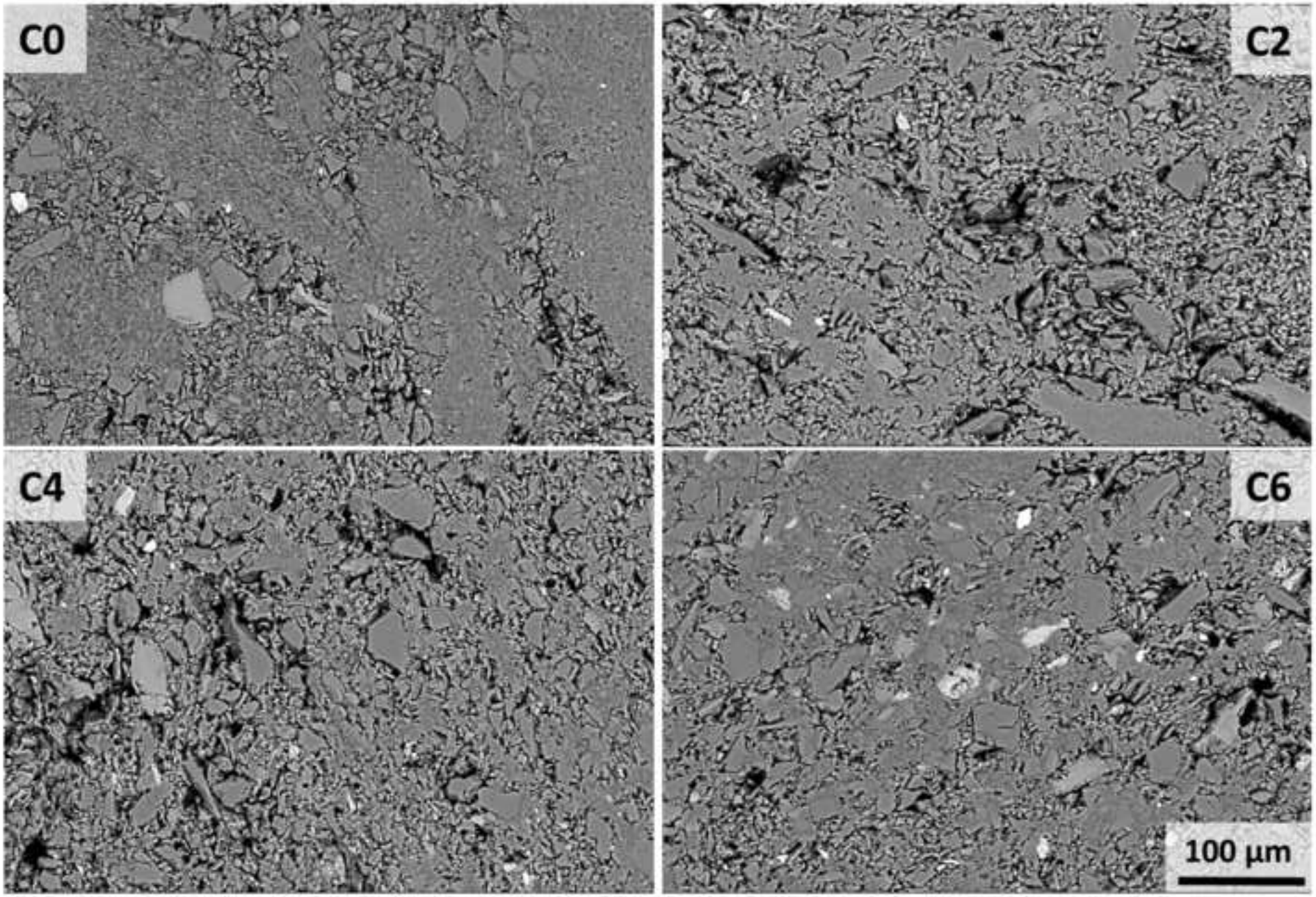

Figure 11

Click here to access/download;Figure;fig11.tiff

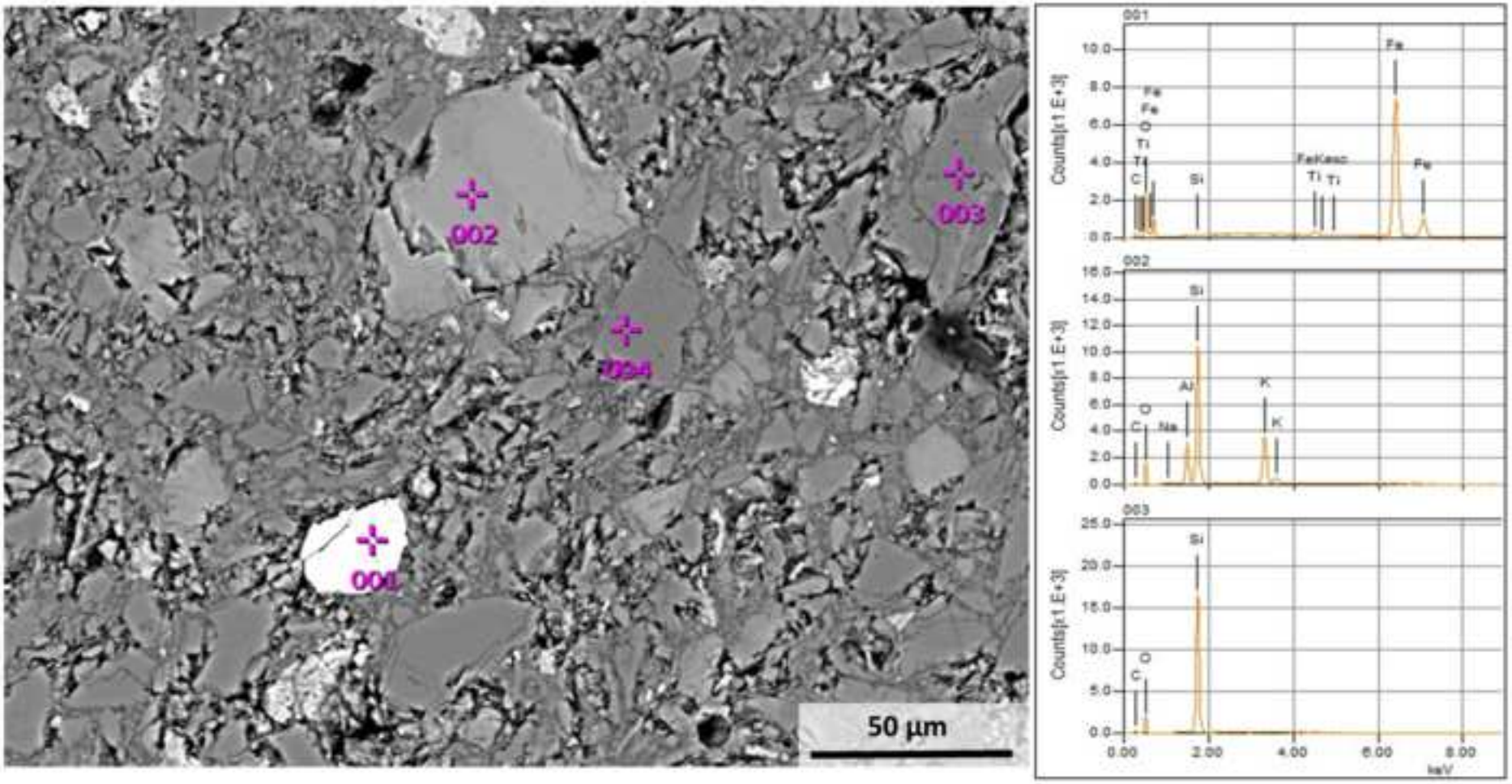

Figure 12

Click here to access/download;Figure;fig12.tiff

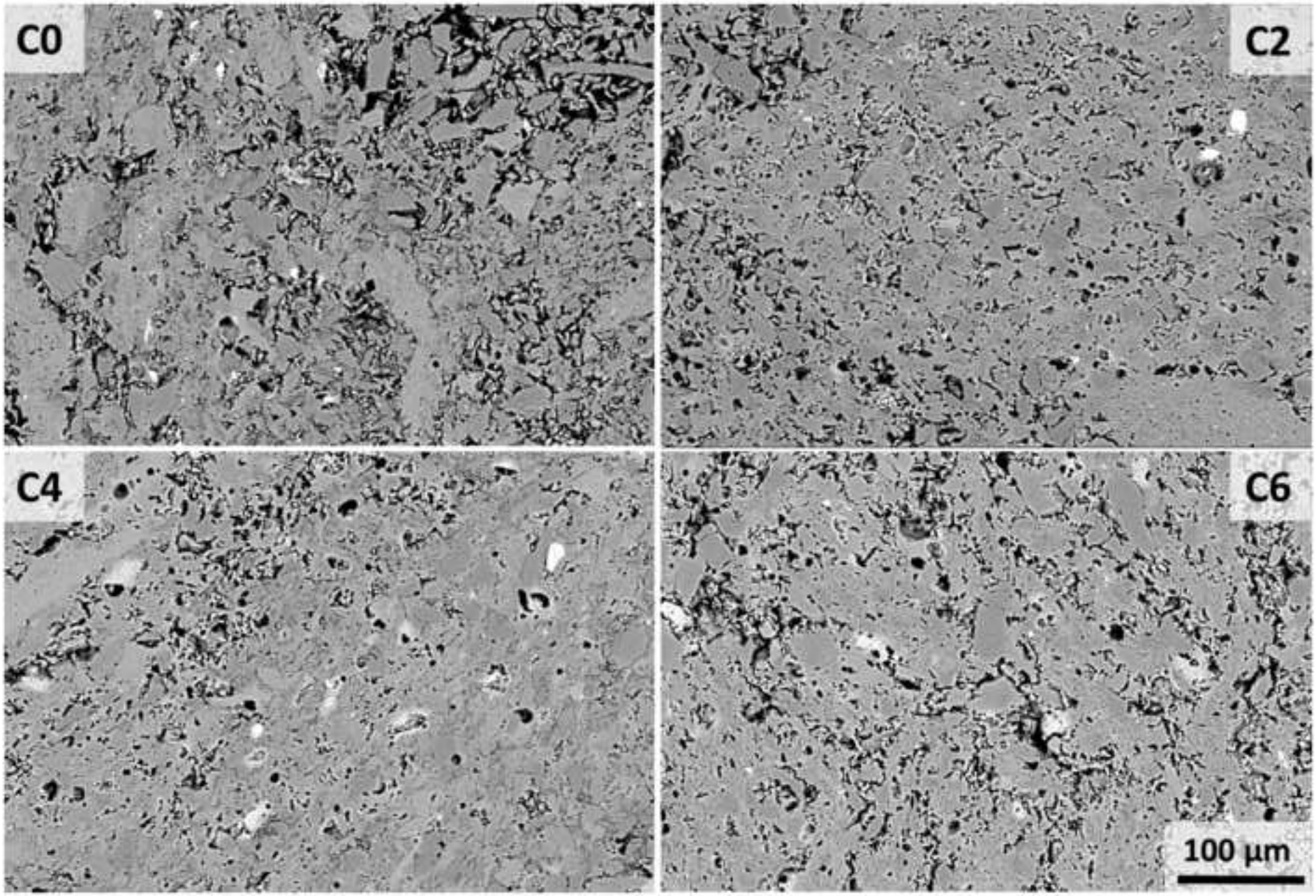

Figure 13

Click here to access/download;Figure;fig13.tiff

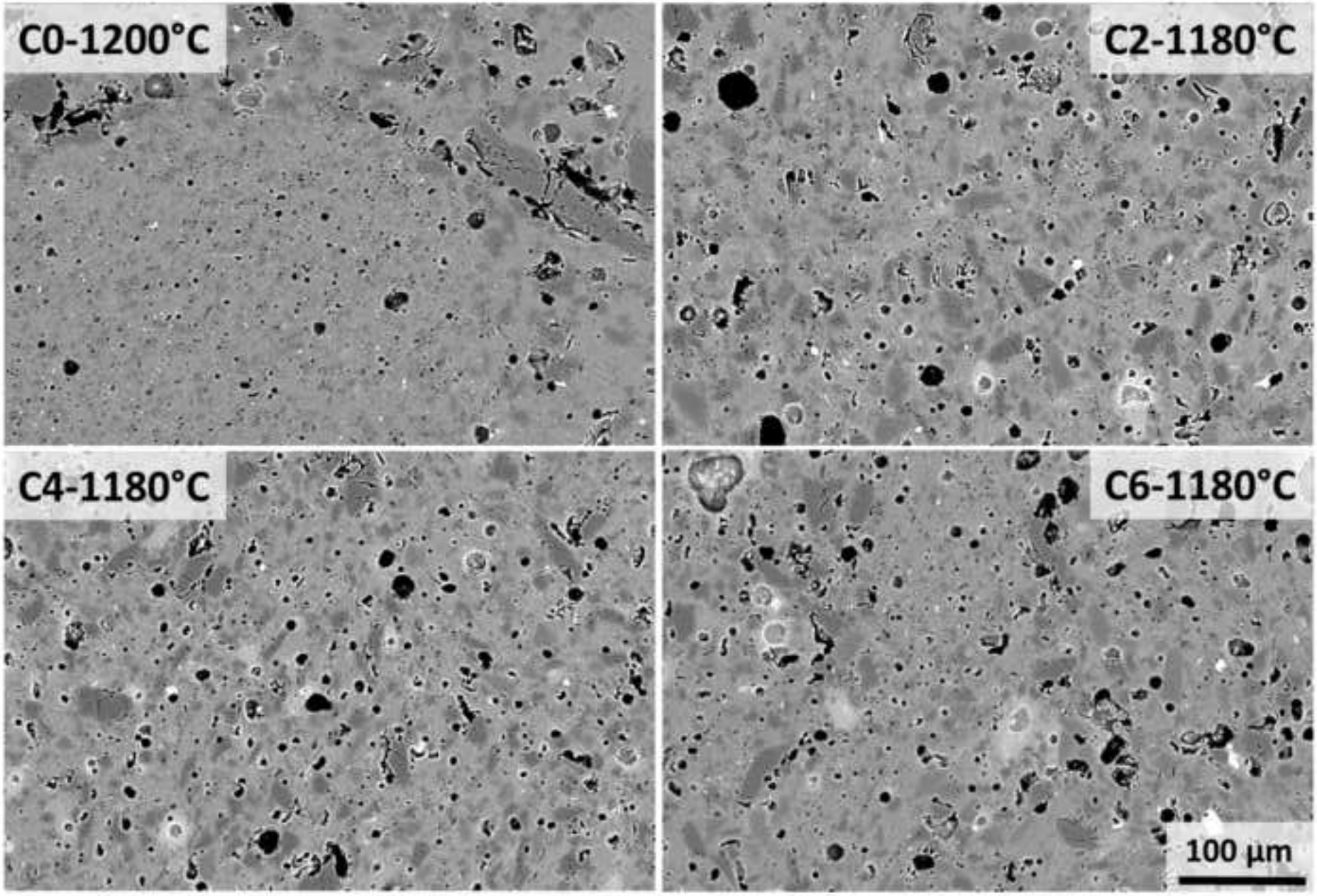

Figure 14

Click here to access/download;Figure;fig14.tiff

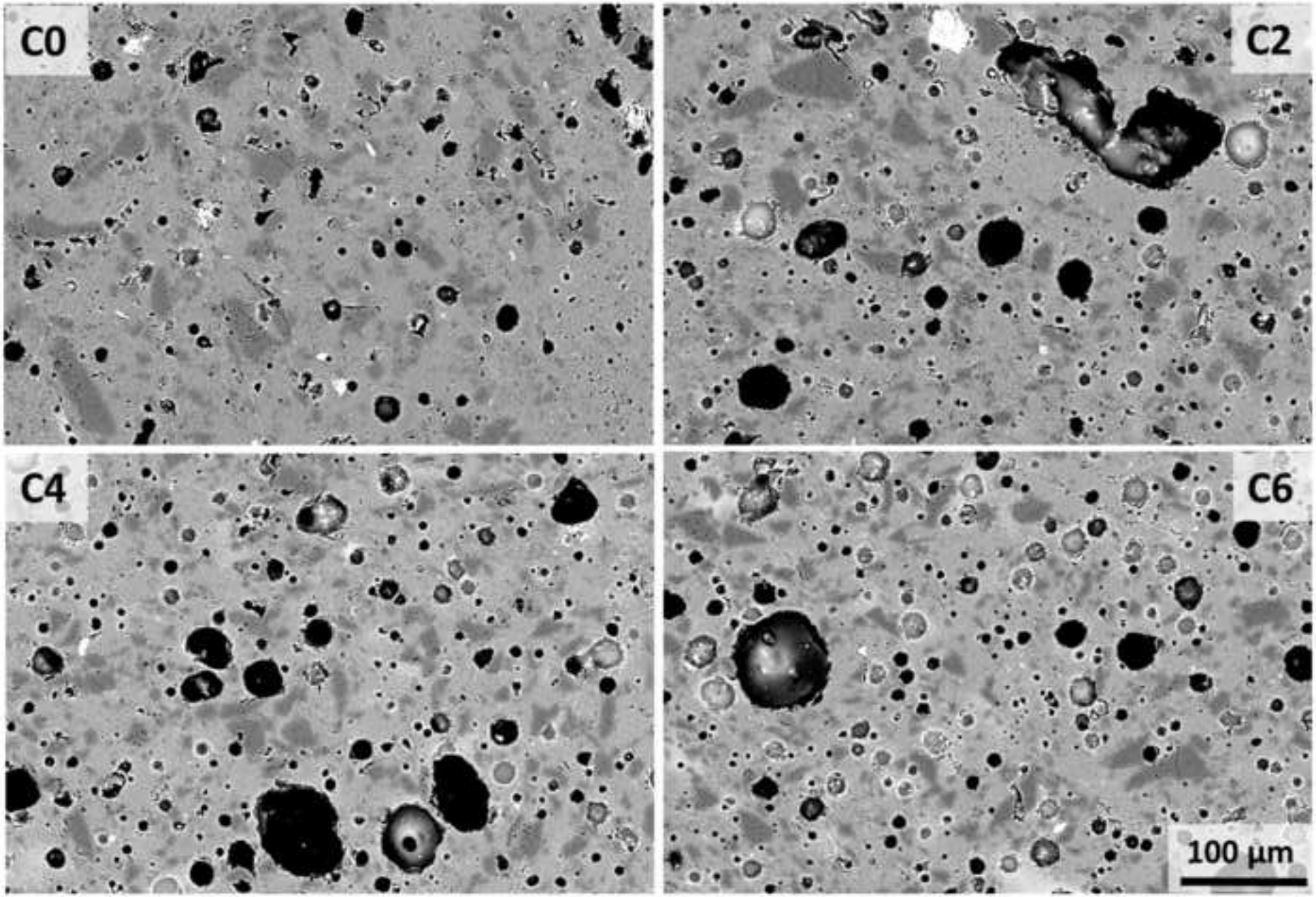

Figure captions

Figure 1. Grain size distribution of BBA

Figure 2. XRPD pattern of the biomass bottom ash under study. Q= Quartz, M=melilite, W= Wollatonite, L=Leucite, P=Portlandite, Cr=Crystobalite, Ca=Calcite, O= Ortoclase.

Figure 3. TGA-DTG curves of BBA

Figure 4. Fusibility of BBA according to the chart after [51].

Figure 5. Particle size distribution of batches C0-C2-C4-C6.

Figure 6. Linear firing shrinkage of finished products fired at different temperatures. Standard deviations within the symbol size.

Figure 7. Gresification curves for batches C0-C2-C4-C6. Standard deviations within the symbol size.

Figure 8. HSM stability curves of C0-C2-C4-C6 bodies.

Figure 9. Phase composition of C0-C2-C4-C6 batches. Standard deviations within the symbol size.

Figure 10. SEM-BS micrographs of C0-C2-C4-C6 bodies fired at 1000°C (scale bar = 100 μm).

Figure 11. SEM-BS micrographs of C6 fired at 1000°C: iron oxide, microcline, quartz (scale bar = 50 μm).

Figure 12. SEM-BS micrographs of C0-C2-C4-C6 bodies fired at 1130°C (scale bar = 100 μm).

Figure 13. SEM-BS micrographs of bodies fired at T_{md} (scale bar = 100 μm).

Figure 14. SEM-BS micrographs of all bodies fired at 1220°C (scale bar = 100 μm).

Declaration of interests

☒ The authors declare that they have no known competing financial interests or personal relationships that could have appeared to influence the work reported in this paper.

☐The authors declare the following financial interests/personal relationships which may be considered as potential competing interests: